Isospin symmetry in nuclear transitions from pion scattering

R. J. Peterson
Nuclear Physics Laboratory, University of Colorado, Boulder, Colorado 80309
(Received 24 February 1993)

A collection of transition matrix elements from pion scattering to natural parity states of spin-zero nuclear targets has been generated from π^+ and π^- inelastic scattering, with results for proton, neutron, and isoscalar transitions, using a consistent reaction model and data from many sources. These are compared to electromagnetic results, to isoscalar results from folding analyses of alpha particle scattering, and to neutron matrix elements inferred by a variety of methods. Good agreement is generally found among these determinations. Comparison of neutron to proton matrix elements shows a simple proportionality to the neutron and proton numbers of the target, reflecting a simple bulk symmetry for a wide range of multipolarities, target masses, and transition strengths.

PACS number(s): 25.80.Ek

I. INTRODUCTION

Stationary states of nuclei may be labeled by their isospin quantum number as a consequence of the isospin invariance of the elementary nucleon-nucleon interaction. Transitions between two such nuclear states show striking isospin selection rules for the special case of electric dipole decays by the coincidence of this operator with that translating the nuclear center of mass. Isospin relations for transitions of other multipolarities are largely uninvestigated, but would be sensitive to a more general dynamic role of isospin invariance. In this work a systematic use of a scattering probe with well-defined isospin sensitivities will show the strong role of nuclear isospin as a dynamic symmetry, in transitions from the ground state to low-lying excited states.

Transitions between nuclear states may, in general, proceed by a coherent combination of isoscalar (ΔT=0) matrix elements M_0 and isovector (ΔT=1) matrix elements M_1, limited by the isospin of 1/2 for the participating nucleons. Alternatively, we may specify proton and neutron amplitudes M_p and M_n. Charge transition amplitudes M_c are reliably available from gamma decay or electron scattering studies, and alpha particle scattering can yield the isoscalar amplitudes. The relations between these have often been compared, usually through comparisons of transition rates or cross sections, and not amplitudes [1]. This loses the coherences between the possible scattering amplitudes. Nonetheless, a large body of scattering data has been analyzed to find consistent patterns of isospin matrix elements for low-lying states of nuclei. Data for first 2^+ states are shown in Ref. [2], for instance.

Instead of comparing noncommensurate probes, it should be preferable to compare π^+ and π^- inelastic scattering, where experimental methods and nuclear distortions are very similar, for the two observables needed to find the two classes of matrix elements [3]. Although some comparisons of these two ways of determining transition matrix elements have been made for isolated examples, there has been no overview to establish the reliabilities of the several methods and to capitalize on the insights from a systematic view. For instance, the transitions in complex nuclei that break isospin symmetry are only to be noted by comparison to many examples of transitions that maintain the symmetry.

In this work a large body of inelastic pion scattering data for M_p and M_n for natural parity (electric) transitions will be compared to values of M_c obtained by electromagnetic transitions and to values of M_0 and M_n inferred from a variety of other methods. A wide range of nuclear targets and transition multipolarities, over a wide range of transition strengths, allows a strong test of the reliability of the results. Proton strengths from the pion work will be compared to electromagnetic data to demonstrate the validity of the method, and the large body of neutron matrix elements obtainable from the pion work will be compared to other results for this less-common observable. Pion data can also be combined for isoscalar matrix elements for comparison to alpha particle data. With these successful comparisons to results from other scattering probes, the pion data for neutron and proton matrix elements of complex nuclei will be compared to demonstrate the dynamic isospin symmetry found in almost all low-lying transitions. A few striking exceptions will be noted; most have been previously discussed.

The rules for pion scattering are simple at beam energies atop the 3-3 resonance, where π^+p (π^-n) amplitudes are three times those for π^+n (π^-p); restated, the probes couple to isoscalar modes with twice the amplitude of that to the isovector. The phases of the couplings with π^+ and π^- differ in relative sign, allowing an "isospin interferometer" to find the matrix elements with good sensitivity. Pion data for the present work were selected from studies at beam energies from 130 to 230 MeV to take advantage of these rules. On complex nuclei these sensitivities are blurred by distortions, so data are compared to distorted-wave impulse approximation (DWIA) calculations to determine the transition strengths, not merely to the simple ratios above. Several versions of these reaction models have been used to present pion results, and where necessary for compatibility, published

 ©1993 The American Physical Society

data have been compared to new distorted-wave impulse approximation (DWIA) calculations in the present work, using a standard model for the nuclear transition. Some data not published in a readily accessible form will also be newly analyzed for the presentations to follow.

Only data on 0^+ target ground states are considered here, and only to natural parity final states. This, and the fact that data will mostly be from small scattering angles, strongly deemphasizes the role of spin-flip transitions. Only transitions with orbital angular momentum of two units or greater are considered, to avoid the very special cases of electric monopole or dipole transitions.

Few pion analyses have treated nuclear Coulomb excitation correctly, as in Ref. [4], but at the resonance this amplitude does not interfere with the strong amplitude, whose real part vanishes at resonance, while the imaginary part of the Coulomb amplitude is always small. The data considered here will thus be little influenced by Coulomb excitation, even when this process was not included explicitly in the analyses.

Most of the transitions considered are to bound states, and of the examples that are unbound to nucleon decay, all will be sharp, long-lived eigenstates. The special cases of broad, high-lying giant resonance transitions will not be dealt with in the present work.

II. REACTION MODELS

Pion scattering reaction models considered here use collective transition densities to treat the bulk properties of the nuclear transition, with a vibrational form for bound states of the form

$$\rho_{\rm tr}(r) = \beta R \; d\rho(r)/dr \tag{1}$$

with $\rho(r)$ the ground state density distribution. Matrix elements are then defined by the relation, for each species μ,

$$M_\mu = \mu \int \rho_{\rm tr}(r) \; r^{L+2} dr/4\pi \quad . \tag{2}$$

The familiar reduced electromagnetic transition probability is then $B(CL) \uparrow = e^2 |M_c|^2$ with the charge matrix element M_c.

Equal proton and neutron density parameters are assumed, with the charge density parameters from elastic electron scattering [5]. Inelastic transitions use the same radial parameters. The small effect of the size distribution of the nucleons has not been applied consistently in the pion analyses, and will be particularly small for the heavy nuclei that form the bulk of the present sample.

Distortions of the reactions have been modeled through the DWIA, using the Kisslinger form of the distorting optical potential. Only first-order calculations, without terms proportional to the square of the density, have been used. Some results of inelastic pion scattering come from analyses that include a small shift of the relative pion-nucleon energy to account for Fermi motion [6]. This has little effect on the extracted transition strengths. The fundamental pion-nucleon coupling is taken from the charge symmetric relations of Rowe, Salomon, and Landau [7], which have also formed the basis of the normalization of many of the scattering experiments themselves. This consistency makes this DWIA procedure even more reliable.

Pion calculations for both charge states were iterated, varying M_p and M_n, until both data sets were fit. The translation between the terminologies is $M_0 = M_n + M_p$ and $M_1 = M_n - M_p$. If data had not been analyzed by these methods in published work, the DWIA calculations were repeated, using the code DWPI [8], to produce the results shown below. From calculations using a deformation length βR for $\mu = Z$, N, $A = N + Z$ or $N - Z$, the matrix elements of order L for vibrations are

$$M_\mu = \mu \beta R \; \frac{L+2}{4\pi} \langle r^{L-1} \rangle . \tag{3}$$

For a uniform distribution of radius R this becomes

$$M_\mu(\text{uniform}) = \mu \frac{3}{4\pi} \beta R^L \quad . \tag{4}$$

Since previous pion work often has given only these βR values, this transformation has sometimes been used to determine the matrix elements presented here, but only for those cases where the usages were clear. The radius R is then taken to be the half-density parameter.

In order to remove trivial size effects, the plots shown in the present work refer to matrix elements in single-particle units (SPU), with

$$\text{SPU} = \frac{3}{L+3} \sqrt{\frac{2L+1}{4\pi}} R^L \tag{5}$$

for a uniform radius $R = 1.2A^{1/3}$ fm. This is also the choice made for compilations of electromagnetic transition rates [9–11]. Electromagnetic transition strengths are taken from compilations whenever possible, with only electron scattering information available for most transitions of order greater than 2. Electric dipole transitions are not included in the present work, since their transition densities are subject to constraints not easily dealt with in a consistent collective model.

Isoscalar transition strengths are taken only from inelastic alpha particle scattering experiments at sufficiently high beam energies to allow a reliable reaction model. Vibrational form factors were used for bound states. Where necessary, new distorted-wave Born approximation (DWBA) calculations were carried out with the optical model parameters of the original works to maintain a method consistent with the pion analyses. The zero-range code DWUCK4 was used for these new computations [12].

Neutron matrix elements M_n have been obtained from a range of methods, including comparison of mirror gamma decays [13, 14], Coulomb-nuclear interference in scattering [15], and indirect comparisons of proton or alpha scattering cross sections to electromagnetic results [16]. No new analysis of these efforts is included in this work.

If uncertainties were not provided for reported experimental matrix elements, a 10% normalization uncertainty in cross sections has been assumed here, for 5% uncertainties in the matrix elements.

Most of the data from other inelastic scattering experiments used for the present comparisons were also analyzed with the collective vibrational form factors. Although consistent with the method used for the pion scattering analysis, there is also the possibility of an incorrect model being used twice, yielding agreement but not a more general truth.

The nucleus ^{12}C has been the best-studied example in pion scattering, at beam energies from 50 MeV to 670 MeV. For this symmetric target it has been found that $M_p = M_n$ for the first 2^+ and 3^- states, as expected for a purely isoscalar vibrational excitation [6]. Figure 1 shows the M_p values for the first 2^+ transition for a wide range of pion beam energies. The constancy of the results across the resonance energies speaks well for the validity of the DWIA methods used to extract these results. Electromagnetic measurements give $M_c = 2.23(0.14)$ SPU [9], very nearly equal to the data points shown in Fig. 1.

III. COMPARISONS OF M_p

Data for pion scattering for 0^+ targets from ^{12}C through ^{208}Pb are presented in Table I for multipolarities 2^+ through 8^+. These entries range in strength from a few tenths of SPU to about 12 SPU. The collective models used for the comparisons are probably not valid for the weaker transitions, and the differing sensitivities to the radial distribution of the transition densities make the comparison particularly unfair for the comparison of pion and electromagnetic results. These are compared in Fig. 2 for the first 2^+ states, expected to be the most collective. A similar plot for 2^+ states in the $f_{7/2}$ shell has been shown for $|M_p|^2$ [18]. Data for 2^+ transitions to states other than the lowest lying are shown in Fig. 3. These are notably noncollective in many cases. Nonetheless, the most striking feature of these two figures is the rather tight correlation observed between charge matrix elements and proton matrix elements from pion scattering. Further comments will follow below.

The 2^+ transitions shown in Fig. 2 are to the lowest-lying 2_1^+ states, most available because of their strength and accessibility. The vibrational model should be appropriate to these pion data, evaluating the strength near the top of the first peak of the angular distribution, near momentum transfer $q = L/R$ fm^{-1}. The electromagnetic data for M_c are determined at the photon point, with much smaller q, but electron scattering results for many states at the top of the form factor have been found to agree with decay data, so the comparison of pion to electromagnetic results is valid, even at the different momentum transfers. The general agreement between matrix elements for the first 2^+ states found in Fig. 2 is like that shown for alpha particle and electromagnetic strengths [1], for transition strengths above about 1 SPU, when scaled by the appropriate number of participating nucleons. A more detailed comparison over a smaller range of masses is presented in Ref. [19] for the first 2^+ states studied by probes largely other than pions.

Higher excitation 2^+ states may have transition densities much different from those of the vibrational model. Nonetheless, use of this simple model is enough to find agreement between pion and electromagnetic (EM) results for many of these weaker transitions. There are some cases in Fig. 3 where $M_p(\pi)$ exceeds M_c(EM) for weaker transitions, indicating perhaps a multistep scattering for the pions or a transition density relatively greater in the surface than that provided by the vibrational model.

For the 2_1^+ states of Fig. 2 the assumption of equal matrix elements for protons (by pion scattering) and charge (by electromagnetic means) results in a χ^2 per degree of freedom ($\chi^2/N_{\rm dof}$) of 4.2. For the higher 2^+ states shown in Fig. 3 $\chi^2/N_{\rm dof}$ is 18, showing the greater role of the exceptional cases. Since a wide range of pion data is included in these comparisons, it is likely that some

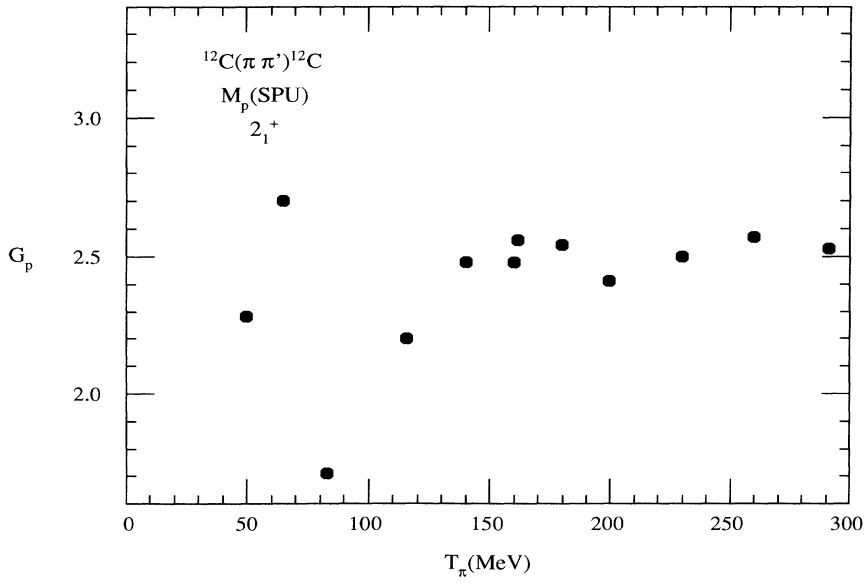

FIG. 1. Proton matrix elements for the first 2^+ transition in ^{12}C as determined over a range of pion beam energies. Data and analysis from Ref. [17] have been used at low energies, and a new DWIA collective analysis of the data from Ref. [6] has been used at and above 100 MeV.

TABLE I. Matrix elements for nuclear transitions are collected, in order of increasing target mass for the 0^+ ground state nuclei for which inelastic pion scattering cross sections have been measured with both π^+ and π^- beams near resonance energy. The index I labels the relative location of the natural parity state listed. Proton and neutron matrix elements have been determined by simultaneous adjustments in a DWIA calculation to match the measured π^+ and π^- cross sections. These matrix elements are in units of fm^L. The ratios of these to the single-particle matrix element are listed as G_p and G_n, with uncertainties. Where the cited reference did not give a specific uncertainty, a 5% range has been listed to reflect the commonly stated 10% uncertainty in the experimental normalizations. References with a "p" denote cases where the pion data shown in the original work have been refit with the standard DWIA method described in the text. This has made possible the extensions of some early work in light of newer spectroscopic information. Some published pion data on light nuclei have been compared only to specific microscopic reaction models, and these have been compared to a consistent collective nuclear model for this table. Cases where inelastic alpha particle scattering analyzed in a folding model have given the isoscalar matrix elements are noted by an "f" in the references. Only those data appear in Figs. 18 and 19. The sum of G_p and G_n from the pion scattering gives the isoscalar sum listed for comparison to the alpha particle results. Electromagnetic determinations of the charge matrix elements are given as ratios to the single-particle standard. Neutron matrix elements determined by a variety of means are also presented with this scale. The figures use data from this table.

	J^π	I	Ex	$M_p(\pi)$	$M_n(\pi)$	$G_p(\pi)$	$G_n(\pi)$	Ref	G_c(em)	Ref	Other G_n	Ref	$G_0(\alpha)$	Ref	$G_0(\pi)$
^{12}C	2^+	1	4.44	7.23	6.77	2.53(0.08)	2.37(0.08)	[6p]	2.23(0.14)	[9]					4.90(0.16)
	3^-	1	9.64	19.0	22.7	2.45(0.10)	2.93(0.10)	"	3.74(0.13)	[10]					5.38(0.20)
	2^+	1	16.1	1.19	1.25	0.42(0.03)	0.44(0.03)	"	0.50(0.03)	"			T=1		(0.86)(0.06)
^{14}C	3^-	1	6.73	13.1	29.5	1.45(0.07)	3.26(0.13)	[40p]	1.55(0.13)	[10]	3.55(0.45)	[10p]	7.97(0.3)	[41]	4.71(0.20)
	2^+	1	7.01	3.22	3.49	1.02(0.05)	1.10	[31]	1.36(0.09)	[9]			4.09(0.4)	"	2.12(0.11)
	2^+	2	8.32	1.65	0	0.52(0.03)	0	"	0.62(0.12)	[30]			3.10(0.2)	"	0.52(0.03)
	3^-	2	10.4	4.36	6.5	0.48(0.02)	0.724	"							1.21(0.06)
^{16}O	3^-	1	6.13	41.9	44.2	4.06(0.20)	4.28(0.21)	[42p]	2.91	[10]			7.46(0.89)	[44f]	8.34(0.41)
	2^+	1	6.92	6.54	6.54	1.89(0.05)	1.89(0.05)	[43p]	1.82(0.09)	[9]			3.10(0.19)	"	3.78(0.10)
	2^+	2	9.85	0.40	1.49	0.11(0.03)	0.43(0.08)	"	0.18(0.01)	"					0.54(0.11)
	4^+	1	10.4	68.4	22.6	2.26(0.19)	0.75(0.05)	"	2.45(0.41)	"					3.01(0.24)
	2^+	3	11.5	4.23	4.33	1.22(0.07)	1.25(0.04)	"	0.95	"			1.22(0.04)	[44]	2.47(0.11)
	3^-	6	15.4	10.2	11.4	0.99(0.09)	1.10(0.06)	"							2.09(0.15)
^{18}O	2^+	1	1.98	5.7	13.9	1.55(0.14)	3.77(0.2)	[45]	1.71(0.04)	[47]	4.30	[45]			5.32(0.34)
	4^+	1	3.55	33.	106.	0.94(0.18)	3.00(0.18)	[46p]	0.88(0.05)	"					3.94(0.36)
	2^+	2	3.92	4.5	6.0	1.20(0.09)	1.60(0.11)	[45]	1.23(0.05)	"	0.83(0.21)	[45]			2.80(0.20)
	3^-	1	5.10	38.5	40.3	3.32(0.17)	3.47(0.17)	[36p]	3.11(0.05)	"					6.79(0.34)
	2^+	3	5.26	5.2	<0.7	1.39(0.11)	<0.19	[45]	1.43(0.04)	"					1.58(0.11)
^{20}Ne	2^+	1	1.63	18.0	18.0	4.48(0.22)	4.48(0.22)	[29]	4.58(0.20)	[9]			9.22(0.16)	[49f]	8.96(0.44)
	4^+	1	4.25	223.	197.	5.45(0.17)	4.82(0.16)	[29p]	4.80(0.52)	[34]			13.8(1.0)	"	10.3(0.33)
	3^-	1	5.62	50.6	50.6	3.93(0.20)	3.93(0.20)	[48]	3.32(0.45)	[10]					7.86(0.40)
	3^-	2	7.16	45.7	45.7	3.55(0.18)	3.55(0.18)	"	1.73	[34]					7.10(0.36)
	2^+	3	7.83	4.07	4.07	1.02(0.06)	1.02(0.06)	"	0.85(0.05)	[28]					2.04(0.10)
	2^+	4	9.00	5.5	5.5	1.37(0.13)	1.37(0.13)	[29]	broad						2.74(0.26)
	4^+	2	9.03	95.	89.	2.33(0.16)	2.17(0.15)	[29p]							4.50(0.31)
	2^+	5	9.49	2.46	2.46	0.62(0.03)	0.62(0.03)	[48]	0.55	[28]					1.24(0.07)
	4^+	3	9.99	84.	84.	2.05(0.45)	2.05(0.45)	[29p]							4.10(0.90)
	5^-	2	10.3	837.	779.	6.50(0.30)	6.06(0.27)	"							12.6(0.57)
	4^+	6	10.8	61.	91.	1.49(0.21)	2.22(0.18)	"							3.71(0.39)
^{22}Ne	2^+	1	1.27	15.2	18.7	3.55(0.23)	4.37(0.30)	[22]	3.53(0.08)	[9]	5.23(1.0)	[22]	3.87(0.09)	[50f]	7.92(0.53)
^{24}Mg	2^+	1	1.37	23.	21.	5.12(0.26)	4.61(0.23)	[51]	4.57(0.07)	[9]			8.83(0.57)	[53f]	9.73(0.49)
	2^+	2	4.24	5.8	5.2	1.28(0.06)	1.15(0.06)	"	1.03(0.05)	[52]			2.44(0.2)	and	2.43(0.12)
	4^+	2	6.01	160.	140.	3.09(0.16)	2.75(0.14)	"	3.98(0.27)	"			7.95(1.04)	[54f]	5.84(0.29)
	3^-	1	7.62	31.	26.	2.00(0.10)	1.70(0.09)	"	2.13(0.20)	"			4.73	"	3.70(0.19)
	3^-	2	8.33	40.	33.	2.57(0.13)	2.13(0.11)	"	2.90(0.19)	"			5.69	"	4.70(0.24)
	4^+	3	9.30	61.	52.	1.17(0.06)	1.00(0.05)	"							2.17(0.11)

TABLE I. (*Continued*).

	J^π	I	Ex	$M_p(\pi)$	$M_n(\pi)$	$G_p(\pi)$	$G_n(\pi)$	Ref	G_c(em)	Ref	Other G_n	Ref	$G_0(\alpha)$	Ref	$G_0(\pi)$
	3^-	3	11.1	18.6	15.2	1.20(0.06)	0.98(0.05)	"	1.61	"			2.28	"	2.18(0.11)
^{26}Mg	2^+	1	1.81	16.8	17.4	3.55(0.2)	3.64(0.2)	[51]	3.64(0.08)	[9]	3.93(0.19)	[22]	7.51	[53f]	7.19(0.40)
	2^+	2	2.94	3.0	8.8	0.63(0.03)	1.84(0.09)	"	0.63(0.08)	[55]			2.82	"	2.47(0.12)
	2^+	3	4.33	1.9	1.9	0.40(0.02)	0.40(0.02)	"	0.338(0.02)	"			0.89	"	0.80(0.04)
	4^+	2	4.90	94.	104.	1.62(0.08)	1.80(0.09)	"	3.32(0.30)	"			3.81	"	2.42(0.17)
	2^+	5	5.29	1.1	3.5	0.23(0.01)	0.73(0.04)	"	0.40(0.03)	"			1.02	"	0.96(0.05)
	4^+	3	5.47	52.	112.	0.90(0.05)	1.93(0.12)	"	1.17(0.15)	"			3.81	"	1.83(0.15)
	4^+	4	5.72	91.	43.	1.57(0.08)	0.74(0.04)	"	2.26(0.40)	"			2.56	"	2.31(0.12)
	3^-	1	6.88	25.	34.	1.49(0.07)	2.05(0.10)	"	1.64(0.15)	"			3.56	"	3.54(0.17)
	3^-	2	7.81	23.5	18.3	1.40(0.07)	1.09(0.05)	"	1.34	"			2.99	"	2.49(0.12)
	3^-	3	8.18	24.4	34.5	1.46(0.08)	2.06(0.10)	"	1.93	"			3.81	"	3.52(0.17)
^{28}Si	2^+	1	1.78	19.1	19.1	3.80(0.04)	3.80(0.04)	[56]	3.58(0.06)	[9]	3.44	[58]	7.08	[58f]	7.60(0.10)
	4^+	1	4.62	95.9	95.9	1.50(0.08)	1.50(0.08)	[57]	2.10(0.12)	[10]			5.14	and	3.00(0.16)
	3^-	1	6.88	61.	61.	3.40(0.17)	3.40(0.17)	"	3.51(0.27)	"			7.01	[53f]	6.80(0.34)
	2^+	2	7.40d	4.1	4.1	0.82(0.02)	0.82(0.02)	[56]	0.72(0.10)	[11][a]			1.43	"	1.64(0.04)
	2^+	4	7.93	2.2	2.2	0.44(0.02)	0.44(0.02)	"	0.55(0.04)	"			1.06	"	0.88(0.44)
^{30}Si	2^+	1	2.24	14.6	17.5	2.77(0.19)	3.33(0.21)	[22]	2.78(0.06)	[9]	3.31(0.15)	[22]			6.10(0.40)
^{34}S	2^+	1	2.13	15.5	17.	2.71(0.17)	2.99(0.19)	[22]	2.54(0.07)	[9]	2.62(0.17)	[14]	2.91(0.24)	[60]	5.70(0.36)
^{40}Ca	3^-	1	3.74	127.	99.	4.94(0.25)	3.85(0.19)	[35p]	5.26	[10]	5.18(0.42)	[16]	10.1	[54f]	8.79(0.44)
	5^-	1	4.49	1230.	1050.	2.62(0.13)	2.25(0.11)	"	3.52	[10]	4.09(0.58)	"	4.69	"	4.87(0.24)
	3^-	2	6.29	50.9	34.5	1.97(0.10)	1.33(0.07)	"	2.14	"			4.05	"	3.30(0.17)
	3^-	3	6.58	61.6	50.4	2.39(0.15)	1.96(0.21)	[35]	1.58	"			3.46	"	4.35(0.36)
	2^+	4	6.91	8.17	5.30	1.28(0.06)	0.83(0.04)	[35p]	1.22(0.12)	"					2.11(0.11)
^{42}Ca	2^+	1	1.52	18.9	22.2	2.87(0.20)	3.38(0.21)	[22]	3.10(0.11)	[9]	4.25(0.45)	[22]	3.53(0.58)	[63p]	6.25(0.41)
	2^+	2	2.42	10.5	8.0	1.59(0.07)	1.22(0.15)	[35p]	1.30(0.19)	[62]			1.62(0.14)	"	2.81(0.22)
	3^-	1	3.45	119.	107.	4.41(0.30)	3.95(0.29)	[61]	4.31(0.10)	"			5.08(0.32)	"	8.36(0.59)
	5^-	1	4.10	2280.	1740.	5.14(0.45)	3.92(0.30)	[35p]	2.40(0.09)	"			4.27(0.27)	"	9.06(0.75)
	3^-	4	4.68	55.7	61.2	2.06(0.08)	2.26(0.21)	"	1.71(0.08)	"					4.32(0.29)
	3^-	5	4.98	39.1	34.3	1.52(0.08)	1.33(0.12)	"	1.17(0.06)	"					2.85(0.20)
	3^-	9	6.30	60.3	29.2	2.23(0.10)	1.08(0.12)	"							3.31(0.22)
^{44}Ca	2^+	1	1.16	20.7	27.7	3.04(0.23)	3.98(0.26)	[35]	3.18(0.07)	[9]			4.77(0.11)	[63p]	7.02(0.49)
	4^+	1	2.28	198.	212.	1.69(0.09)	1.82(0.09)	[64]	1.63(0.05)	[65]					3.51(0.17)
	2^+	2	2.66	7.4	5.1	1.09(0.06)	0.75(0.04)	"	1.31(0.06)	[66]			1.35(0.09)	"	1.84(0.09)
	3^-	1	3.31	98.	98.	3.44(0.24)	3.21(0.23)	[35]	3.44(0.16)	[62]			4.80(0.15)	"	6.65(0.47)
	5^-	1	3.91	1260.	1100.	2.64(0.28)	2.30(0.25)	[35p]	2.05(0.09)	"			2.84(0.36)	"	4.94(0.53)
	3^-	3	4.40	45.1	67.6	1.59(0.09)	2.38(0.12)	"	1.49(0.08)	"			2.95(0.12)	"	3.97(0.21)
^{48}Ca	2^+	1	3.83	11.2	26.7	1.56(0.16)	3.71(0.22)	[35]	1.27(0.21)	[9]	4.02(0.61)	[61]	3.79(0.22)	[63p]	5.27(0.38)
	3^-	1	4.51	96.9	111.	3.13(0.23)	3.57(0.25)	"	2.90(0.10)	[67]			5.59(0.21)	"	6.70(0.48)
	3^-	2	5.37	46.3	46.3	1.50(0.08)	1.49(0.14)	[35p]	1.33(0.04)	"			2.24(0.20)	"	2.99(0.22)
	5^-	1	5.73	1740.	1060.	3.15(0.30)	1.92(0.24)	"	2.70	"			3.03(0.61)	"	5.07(0.54)
	3^-	3	7.66	53.2	61.8	1.72(0.06)	2.00(0.12)	"	1.75(0.06)	"					3.72(0.19)
^{48}Ti	2^+	1	0.98	26.3	31.5	3.66(0.14)	4.38(0.10)	[68]	3.72(0.10)	[9]			8.33	[70]	8.04(0.24)
	4^+	1	2.30	197.	228.	1.50(0.14)	1.74(0.21)	"	1.84(0.04)	[69]					3.24(0.35)
	2^+	2	2.42	7.56	5.83	1.05(0.10)	0.81(0.15)	"	1.12(0.13)	"			2.30	"	1.86(0.25)
	4^+	2	3.24	356.	457.	2.71(0.17)	3.48(0.27)	"					5.95	"	6.19(0.44)
	3^-	1	3.36	67.	73.	2.17(0.10)	2.36(0.14)	"					4.23	"	4.53(0.24)

TABLE I. (*Continued*).

	J^π	I	Ex	$M_p(\pi)$	$M_n(\pi)$	$G_p(\pi)$	$G_n(\pi)$	Ref	G_c(em)	Ref	Other G_n	Ref	$G_0(\alpha)$	Ref	$G_0(\pi)$
	2^+	3	3.37	8.2	7.6	1.14(0.12)	1.05(0.09)	"	1.21(0.08)	[71]					2.19(0.21)
	2^+	4	3.62	5.8	7.1	0.81(0.04)	0.98(0.06)	[68p]	0.52(0.03)	"					1.79(0.10)
	3^-	2	3.85	53.2	53.5	1.72(0.07)	1.73(0.21)	[68]					3.00	"	3.45(0.28)
	2^+	5	4.05	6.28	7.31	0.87(0.15)	1.02(0.07)	[68p]							
	4^+	3	4.39	118.	251.	0.90(0.15)	1.91(0.22)	[68]							2.81(0.37)
	3^-	3	4.58	49.2	50.4	1.59(0.10)	1.63(0.19)	"					3.75	"	3.22(0.29)
	2^+	6	4.92	5.4	6.0	0.75(0.14)	0.84(0.08)	[68p]	0.52(0.04)	[71]			1.78	"	1.59(0.22)
	4^+	4	5.15	121.	274.	0.92(0.10)	2.09(0.20)	"					2.61	"	3.01(0.30)
	3^-	5	5.52	35.3	43.9	1.14(0.06)	1.42(0.06)	"							2.56(0.12)
^{50}Ti	2^+	1	1.55	18.9	16.6	2.56(0.11)	2.24(0.09)	[68]	2.30(0.16)	[9]			4.80	[73]	4.80(0.20)
	4^+	1	2.68	231.	222.	1.67(0.22)	1.60(0.20)	"	2.17(0.03)	[72]			4.02	"	3.27(0.42)
	2^+	2	4.17	2.29	7.91	0.31(0.16)	1.07(0.10)	"							1.38(0.26)
	2^+	3	4.31	8.14	8.21	1.10(0.20)	1.11(0.13)	"	0.97	"					2.21(0.33)
	3^-	1	4.41	68.	66.	2.12(0.10)	2.04(0.13)	"	1.94(0.04)	"			4.98	"	4.16(0.25)
^{52}Cr	2^+	1	1.43	24.3	21.8	3.19(0.06)	2.87(0.06)	[68]	3.37(0.08)	[9]			6.33(0.55)	[63p]	6.06(0.12)
	4^+	1	2.37	257.	253.	1.76(0.13)	1.73(0.16)	"	1.84(0.16)	[69]			2.92(0.27)	"	3.49(0.29)
	4^+	2	2.77	223.	244.	1.53(0.08)	1.67(0.14)	"	1.51	[74]			2.54(0.32)	"	3.20(0.22)
	2^+	3	3.16	9.98	11.0	1.31(0.04)	1.45(0.05)	[68p]	0.46(0.04)	"			1.66(0.08)	"	2.76(0.10)
	4^+	3	3.41	97.3	203.	0.67(0.02)	1.39(0.08)	"							2.06(0.10)
	2^+	4	3.77	9.75	14.3	1.29(0.05)	1.88(0.06)	[68]	1.32(0.09)	"			2.48(0.06)	"	3.17(0.11)
	3^-	1	4.56	82.7	83.	2.47(0.09)	2.48(0.09)	"	2.47(0.06)	"			3.89(0.10)	"	4.55(0.18)
	4^+	5	4.63	359.	188.	2.46(0.33)	1.29(0.19)	"							3.75(0.52)
^{54}Fe	2^+	1	1.41	21.7	21.6	2.80(0.12)	2.78(0.10)	[68]	3.19(0.13)	[9]	3.37	[75]	4.17(0.15)	[63p]	5.58(0.22)
	4^+	1	2.54	304.	183.	1.98(0.16)	1.19(0.10)	"	2.16	[72]			3.06(0.13)	"	3.17(0.26)
	2^+	2	2.96	12.7	18.9	1.63(0.09)	2.43(0.10)	"	1.45(0.10)	and			2.96(0.10)	"	4.06(0.19)
	2^+	3	3.17	10.3	8.0	1.32(0.15)	1.03(0.14)	"	0.85(0.09)	[69]			1.71(0.10)	"	2.35(0.29)
	4^+	2	3.30	137.	264.	0.89(0.10)	1.72(0.13)	"					1.76(0.16)	"	2.61(0.23)
	4^+	3	3.83	342.	310.	2.23(0.22)	2.02(0.19)	"					2.74(0.11)	"	4.25(0.41)
	4^+	4	4.05	124.	156.	0.81(0.11)	1.02(0.17)	[68p]	1.94(0.09)	"			1.44(0.18)	"	1.83(0.28)
	4^+	7	4.29	172.	227.	1.12(0.08)	1.48(0.20)	"					2.16(0.07)	"	2.60(0.8)
	2^+	4	4.58	6.85	6.85	0.88(0.14)	0.88(0.12)	[68]					1.37(0.06)	"	1.76(0.26)
	3^-	1	4.78	62.7	54.7	1.80(0.09)	1.57(0.17)	"	1.90	"			2.34(0.04)	"	3.37(0.26)
	3^-	2	5.62	8.4	37.3	0.24(0.04)	1.07(0.23)	"							1.31(0.27)
	3^-	4	6.40	91.6	81.8	2.63(0.10)	2.35(0.20)	"	2.24	"			3.37(0.23)	"	4.98(0.30)
^{56}Fe	2^+	1	0.85	30.8	35.3	3.85(0.08)	4.43(0.10)	[68]	3.91(0.08)	[9]	4.34	[75]	8.51(0.35)	[50f]	8.28(0.18)
	4^+	1	2.09	100.	161.	0.62(0.21)	1.00(0.17)	"	1.27(0.08)	[69]					1.62(0.34)
	2^+	2	2.66	8.72	13.2	1.08(0.09)	1.65(0.10)	"	0.52(0.07)	"					2.73(0.19)
	2^+	3	2.96	7.34	9.25	0.92(0.15)	1.16(0.20)	[68p]	0.40(0.06)	"					2.08(0.35)
	4^+	2	3.12	400.	432.	2.48(0.13)	2.68(0.29)	[68]							5.16(0.42)
	2^+	4	3.37	9.11	10.1	1.14(0.08)	1.27(0.12)	"	0.28(0.05)		"				2.41(0.20)
	4^+	3	4.12	219.	238.	1.36(0.06)	1.48(0.11)	[68p]							2.84(0.17)
	3^-	1	4.51	112.	150.	3.10(0.08)	4.14(0.12)	"	3.61	"			6.85(0.41)	[50f]	7.24(0.20)
	5^-	1	5.12	1230.	1750.	1.72(0.21)	2.44(0.32)	"							4.16(0.53)
^{58}Ni	2^+	1	1.45	22.4	31.4	2.74(0.27)	3.85(0.39)	[32]	3.05(0.07)	[9]	4.13	[16]	6.70(0.10)	[76f]	6.59(0.66)
	3^-	1	4.47	104.	144.	2.78(0.28)	3.84(0.38)	"	2.70(0.05)	[69]	3.32(0.42)	"	6.58(0.6)	"	6.62(0.66)
^{60}Ni	2^+	1	1.45	18.2	18.9	2.18(0.22)	2.26(0.23)	[32]	3.36(0.05)	[9]	3.73	[72]	8.84(0.26)	[50f]	4.44(0.44)

TABLE I. (*Continued*).

	J^π	I	Ex	$M_p(\pi)$	$M_n(\pi)$	$G_p(\pi)$	$G_n(\pi)$	Ref	G_c(em)	Ref	Other G_n	Ref	$G_0(\alpha)$	Ref	$G_0(\pi)$
	3^-	1	4.01	134.	117.	3.47(0.35)	3.02(0.30)	"	2.71(0.15)	[69]			10.5(1.2)	[77f]	6.49(0.65)
^{62}Ni	2^+	1	1.17	34.7	48.6	4.06(0.41)	5.69(0.57)	[32]	3.30(0.02)	[9]	3.80	[72]	10.1(1.1)	[77]	9.75(0.98)
	3^-	1	3.78	188.	207.	4.69(0.47)	5.17(0.52)	"	2.93(0.05)	[69]			12.5(1.5)	"	9.86(0.99)
^{64}Ni	2^+	1	1.35	25.9	45.5	2.97(0.30)	5.22(0.52)	[32]	2.98(0.02)	[9]	3.62	[72]	8.45(1.0)	[77]	8.19(0.82)
	3^-	1	3.56	150.	241.	3.64(0.36)	5.85(0.59)	"	3.46(0.02)	[78]			9.78(1.3)	"	9.49(0.95)
^{90}Zr	2^+	1	2.19	34.	32.	3.11(0.16)	2.92(0.15)	[38]	2.29(0.09)	[66]	2.63(0.10)	[16]	5.24	[79f]	6.03(0.31)
	3^-	1	2.75	348.	302.	6.00(0.30)	5.20(0.26)	"	5.00(0.30)	"	5.23(0.25)	"	11.9	"	11.2(0.56)
^{104}Pd	2^+	1	0.56	69.	95.	5.73(0.17)	7.88(0.25)	[25]	6.05(0.20)	[15]	7.06	[15]	13.1(0.6)	[15f]	13.6(0.42)
	3^-	1	2.19	365.	542.	5.44(0.13)	8.08(0.21)	"	"			"	14.4(0.7)	"	13.5(0.34)
^{106}Pd	2^+	1	0.51	74.	106.	6.06(0.17)	8.68(0.24)	[25]	6.62(0.18)	[15]	9.01	[15]	15.4(0.8)	[15f]	14.7(0.4)
	3^-	1	2.08	360.	533.	5.27(0.13)	7.80(0.21)	"	5.00	"	9.30	"	14.3(0.7)	"	14.1(0.4)
^{108}Pd	2^+	1	0.43	80.	122.	6.47(0.17)	9.87(0.24)	[25]	7.03(0.18)	[15]	9.87	[15]	16.85(0.9)	[15]	16.3(0.5)
	3^-	1	2.05	334.	539.	4.80(0.11)	7.74(0.19)	"	4.36	"	7.46	"	11.83(0.6)	"	12.5(0.30)
^{110}Pd	2^+	1	0.37	88.	140.	7.03(0.16)	11.2(0.3)	[25]	7.43(0.17)	[15]	9.27	[15]	16.6(0.8)	[15]	18.2(0.5)
	3^-	1	2.04	315.	523.	4.44(0.11)	7.37(0.18)	"	4.12	"	6.47	"	10.59(0.5)	"	11.8(0.3)
^{118}Sn	2^+	1	1.23	58.	84.	4.42(0.22)	6.45(0.33)	[38]	3.48(0.07)	[80]	6.30(0.10)	[16]	7.53(0.07)	[76f][b]	10.9(0.54)
	3^-	1	2.33	448.	575.	5.89(0.29)	7.56(0.38)	"	4.36	"	7.89(0.13)	"	9.78(1.0)	"	13.5(0.67)
^{152}Sm	2^+	1	0.12	184.	202.	11.9(0.39)	18.9(2.6)	[81]	11.9(0.07)	[9]			7.67	[82]	30.8(3.9)
	3^-	1	1.04	434.	557.	4.31(0.15)	5.44(0.16)	"	3.65(0.26)						9.75(0.31)
^{206}Pb	2^+	1	0.80	30.9	77.3	1.63(0.08)	4.07(0.20)	[83]	1.69(0.02)	[84]	4.16	[83]	3.43	[83]	5.70(0.28)
	3^-	1	2.65	(782.)	1180.	(5.88)[c]	8.90(0.45)	"	5.88	"	8.90	"	10.98	"	14.8(0.5)
	2^+	9	4.11	(50.)	75.6	(2.63)[c]	3.98(0.20)	"	2.63	"	3.98	"			6.61(0.3)
^{208}Pb	3^-	1	2.61	759.	1470.	5.66(0.2)	10.98(0.5)	[20]	5.88(0.07)	[21]	10.2	[21]	15.7(0.80)	[49f]	16.6(0.7)
	5^-	1	3.20	1.99E4	4.31E4	3.13(0.07)	6.67(0.3)	and	3.31	and	6.26	"	7.66	[85]	9.80(0.4)
	5^-	2	3.71	1.30E4	2.73E4	2.05(0.2)	4.2(0.4)	[21]	2.43	[85]	4.15	"	4.71	"	6.25(0.6)
	2^+	1	4.08	51.5	93.5	2.69(0.2)	4.90(0.1)	"	2.81(0.14)	"	5.89	"	6.85(0.19)	[76f]	7.59(0.3)
	4^+	1	4.32	3830.	6280.	4.14(0.3)	6.77(0.4)	"	4.25	"	7.38	"	8.41	[85]	10.9(0.7)
	6^+	1	4.42	1.99E5	3.07E5	4.58(0.44)	7.0(0.3)	"	5.89	"	8.42	"	5.91	"	11.6(0.7)
	8^+	1	4.61	6.80E6	15.8E6	3.28(0.16)	7.63(0.38)	"	3.55	"	8.72	"			10.9(0.5)
	3^-	2	4.70	256.	402.	1.91(0.10)	3.00(0.15)	"							4.91(0.25)
	3^-	3	5.30	290.	474.	2.16(0.11)	3.53(0.18)	"	2.68	"					5.69(0.3)

[a] Two electromagnetic transition rates have been added to compare to the unresolved doublet in pion scattering.

[b] The alpha particle data are for ^{120}Sn.

[c] The pion analysis fixed the proton matrix element to the electromagnetic value.

uncertainties are underestimated. A 5% uncertainty has been assumed where no other information was available; these are listed in Table I.

Nuclear octupole excitations by pion scattering have been mainly to the first 3^- states, so again the vibrational model should be valid. Figure 4 shows the comparison of proton matrix elements for pions and EM processes for these prominent first vibrational states. Most of the latter are from electron scattering, so the comparisons are generally at the same momentum transfers. Good agreement between the two classes of determinations seems to be found. The $\chi^2/N_{\rm dof}$ is 5.1 for the assumption that proton and charge matrix elements are equal for the first 3^- states, subject to the incomplete knowledge of the uncertainties in the pion data. Transitions to 3^- states other than the lowest lying are found in Fig. 5 for electromagnetic and pion scattering. These are more closely equal than was found for the higher 2^+ states in Fig. 3.

Multipole transitions of order 4 and greater are quite scarce in the pion data, and the suitability of the vibrational model is not obvious. The most carefully studied high multipole (to 8^+) example is ^{208}Pb, where two pion experiments agree quite closely in their conclusions at different beam energies [20, 21]. Figure 6 shows the com-

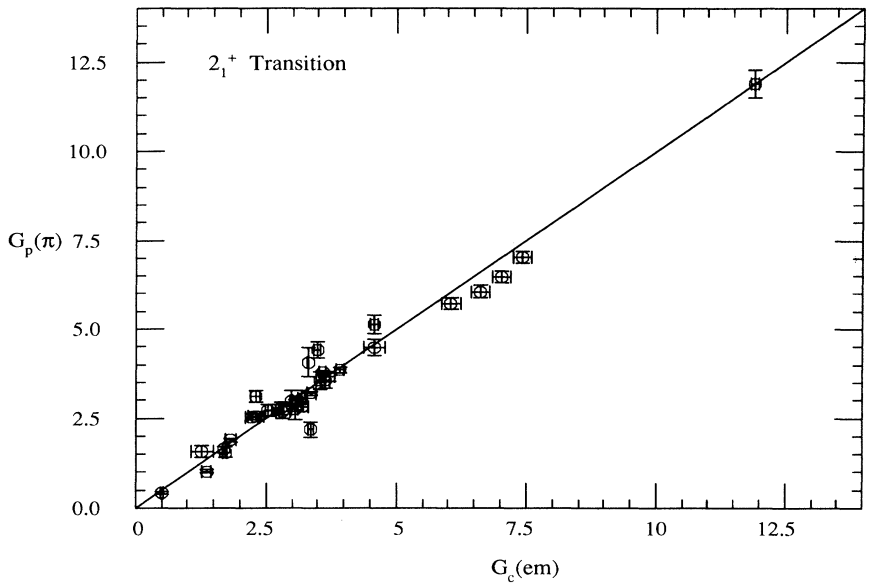

FIG. 2. Matrix elements in SPU for protons, determined by pion scattering, and for charge, determined by electromagnetic methods, are compared for the first 2^+ states of many nuclei. Data and references are in Table I. The line is for equal values.

parison for M_p for pions and M_c for electron scattering for multipolarities of four and greater. Several 4^+ transitions are known for some nuclei in this sample.

IV. NEUTRON MATRIX ELEMENTS

Negative pion scattering has the greatest leverage in determining M_n, and since π^- beam intensities are less than π^+, these data points often have larger uncertainties. Neutron matrix elements M_n are derived from the same simultaneous analysis as M_p, adjusting the transition strengths in a DWIA calculation to achieve agreement with data for both charge states. These values, either from the original work or as reanalyzed for consistency, are listed in Table I for pion scattering on many nuclei.

Under the assumption of charge symmetry, comparison of EM decay rates in $T = 1$ mirror nuclei can provide values of M_c for electric transitions that can provide separate values of M_p and M_n [13, 14]. A detailed comparison for 2_1^+ transitions for $A = 18$–42 between these data and pion data is found in Ref. [22], and the derived values of M_n(EM) are listed in Table I for comparison to $M_n(\pi)$ for this limited sample.

Inelastic alpha particle scattering at small angles excites nuclear transitions by a coherent mixture of Coulomb and isoscalar amplitudes. Suitable analysis can

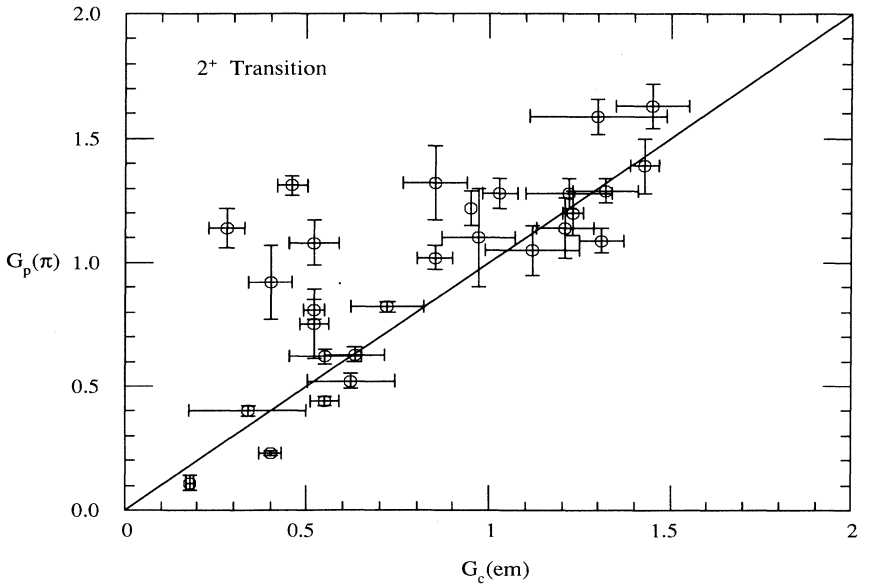

FIG. 3. As Fig. 2, but for 2^+ transitions other than the lowest lying.

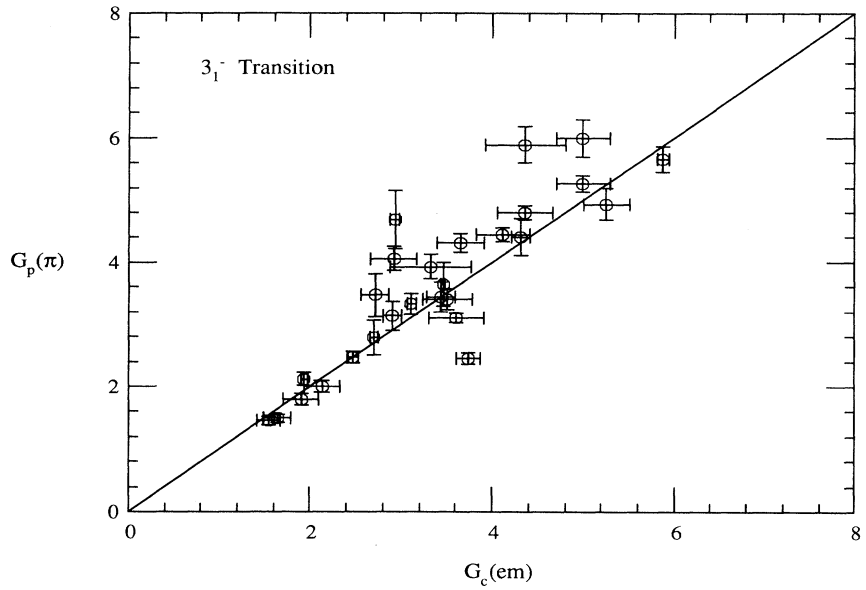

FIG. 4. As Fig. 2, but for the lowest 3^- states.

then determine both and these have been presented also as neutron and proton matrix elements. Results for those cases common also to pion data are compared in Table I. Determinations of these amplitudes from scattering of heavy ions have also been made (for instance in Ref. [23]), but only alpha particle scattering measurements are listed here.

Another means to determine neutron matrix elements is by the isovector (p,n) charge exchange reaction to analogs of the target states, compared to proton inelastic scattering. Combining these can yield the neutron matrix elements, and a few cases in common with pion scattering are listed in Table I.

A less sensitive and more model-dependent extraction of M_n can be performed by comparing incoherent cross sections, not amplitudes, for proton scattering to electron scattering. These results have been compared in detail to those from pion scattering for ^{208}Pb in Ref. [21], with numerical results listed in Table I together with other cases. Most of these analyses of two probes use the collective vibrational model of the transition at least once.

Although the comparisons of neutron matrix elements from various methods are not necessarily of the same sensitivity or reliability, the scattered results in Table I do show general agreement. Figure 7 shows a comparison of pion results to those of other methods for the first

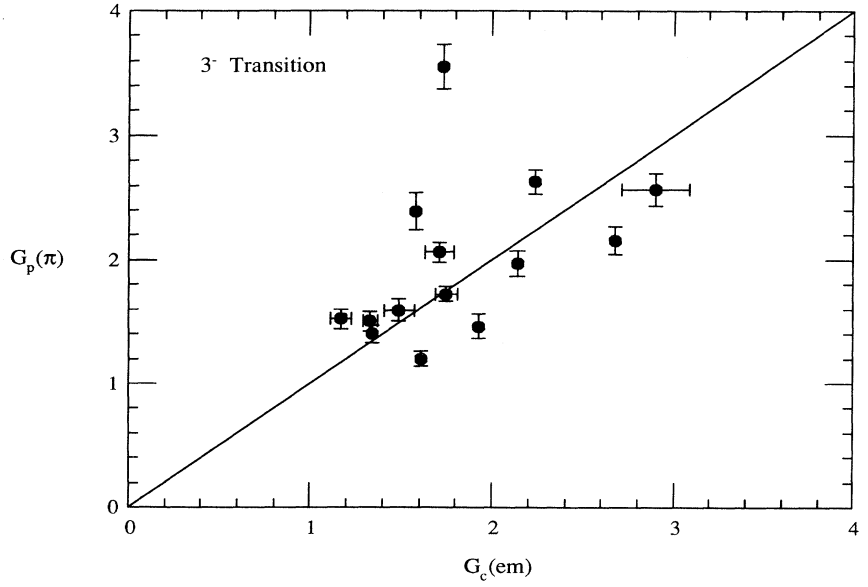

FIG. 5. As Fig. 2, but for 3^- transitions to other than the lowest-lying states.

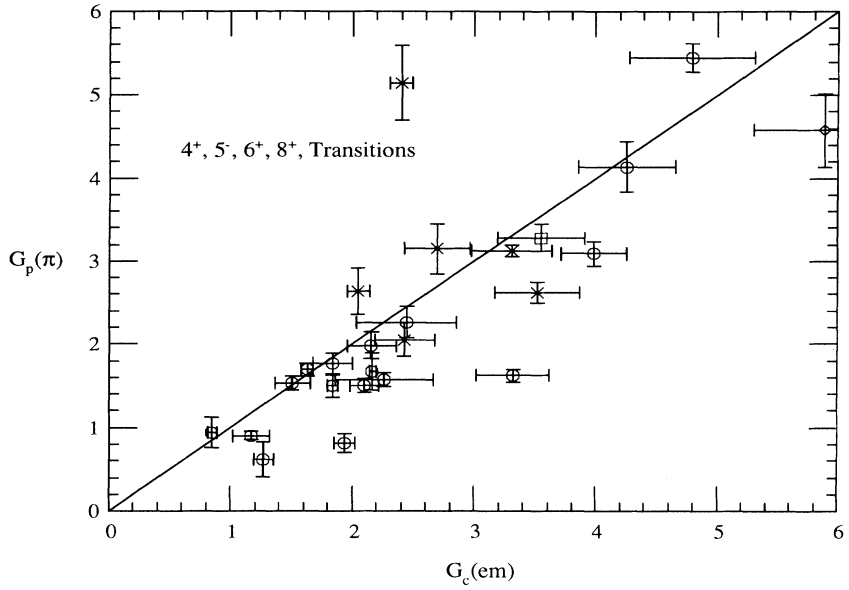

FIG. 6. As Fig. 2, but for multipolarities greater than three. Symbols are circles for 4^+, crosses for 5^-, diamonds for 6^+, and squares for 8^+ transitions.

2^+ states of a number of nuclei, all with at least two single-particle units of transition amplitude. Quite good agreement is found, without any preference for any of the methods alternative to pion scattering. An assumed equality of neutron matrix elements from pions to the other means yields a $\chi^2/N_{\rm dof}$ of 5.8.

The pion data for neutron and proton matrix elements are plotted in Figs. 8–12, as the ratios of the number of single-particle units per nucleon. In the limit of an overall nuclear oscillation, these quantities would be equal.

The simple isospin symmetry is indeed found for the first 2^+ states seen in Fig. 8, with ^{18}O as the exception. This, and other departures from the general trends, will be treated in Sec. VI.

Higher 2^+ states may be expected in some cases to show an isospin reversal relative to the lowest 2^+ transition [19]. This will be revealed most sensitively in the pion scattering, as in Fig. 9. The diagonal line is the expectation of an isospin symmetry, which agrees with most of the cases shown, even for 2^+ states other than the lowest. Exceptions, some of them very striking, will be discussed in Sec. VI.

The first 3^- data for neutrons and proton matrix elements are shown in Fig. 10, and found to match quite closely the symmetric expectation. This is also very much the case with higher 3^- states, as shown in Fig. 11.

For multipolarities greater than three, collective features may be expected to be less dominant, and the hy-

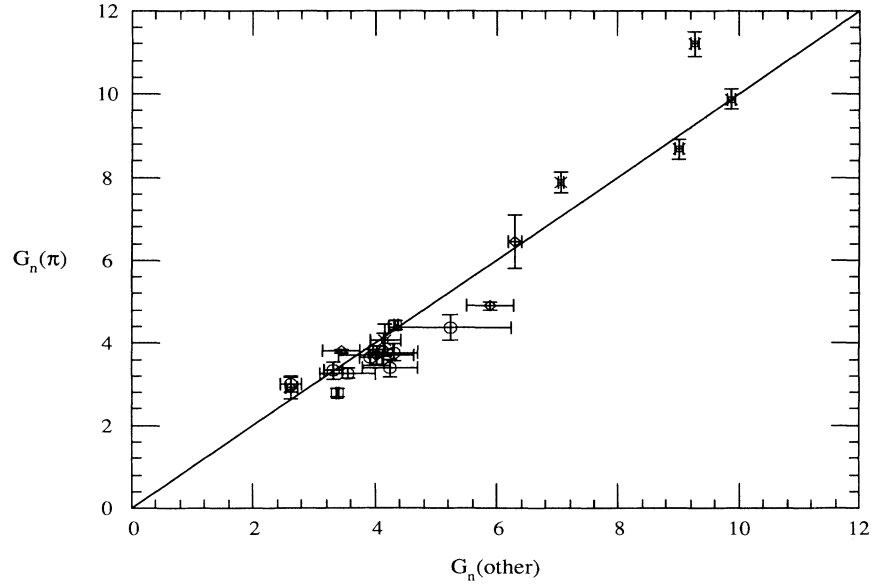

FIG. 7. Neutron matrix elements for lowest-lying 2^+ state of many nuclei are compared for pion scattering and other means. Electromagnetic results for $T = 1$ nuclei are shown by circles, nuclear Coulomb interference results are shown by stars, comparisons of (p,n) and (p,p') by squares, and comparisons of proton and electron scattering yield points shown by diamonds. Specific cases are found in Table I.

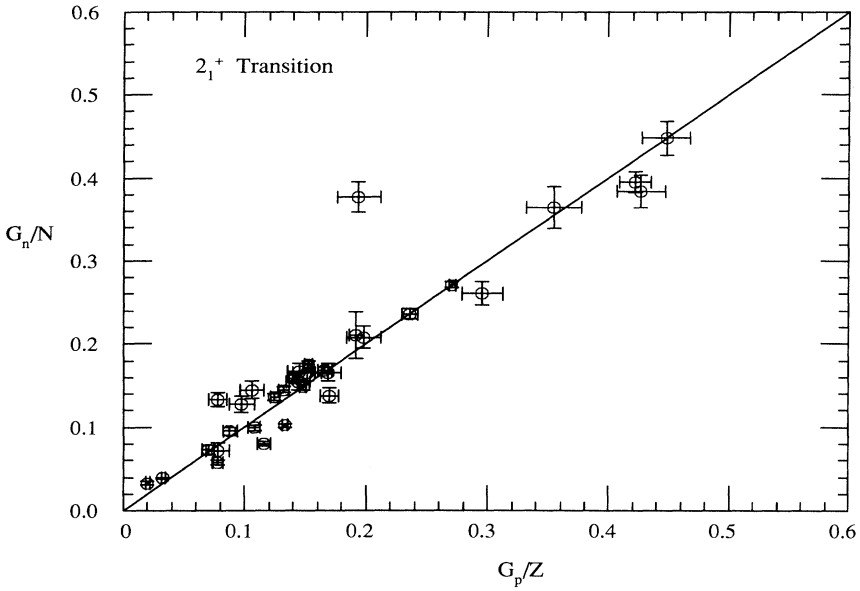

FIG. 8. Matrix elements as determined by pion inelastic scattering are compared for proton and neutron components, divided by the number of protons and neutrons. These points are for the lowest-lying 2^+ states of the nuclei studied. A uniform hydrodynamic oscillation would give equal values, as indicated by the diagonal line.

drodynamic model less appropriate. Figure 12 shows the diagonal symmetric line to agree quite well for spins of up to 8^+.

These same pion data, expressed as the ratio of single-particle units per nucleon, are plotted against the target masses in Figs. 13–17. The same exceptional cases are noted by departures from unity. No particular pattern of deviations from the hydrodynamic model is noted, except that the few cases found are usually associated with at least one closed shell.

V. ISOSPIN MATRIX ELEMENTS

Pion-induced scattering results with both charge states can also be combined to form the isoscalar transition matrix elements $M_0(\pi)$ for comparison to results from alpha scattering $M_0(\alpha)$. Previous comparisons of $M_0(\alpha)$ to electromagnetic data have used the uniform hydrodynamical model, which gives $M_0 = AM_p/Z$ [1]. Pion and alpha data are compared through observations at the first maximum, and thus at the same momentum transfers.

Comparisons of alpha scattering data and electromagnetic data are quite common, and pion and electromagnetic results are in generally good concord. Since there are often simplifying assumptions made for the radial distributions treated in the alpha particle scattering, only those cases treated with folding methods will be compared to the pion data in the figures.

Isoscalar transition amplitudes, in single-particle units, are shown in Fig. 18 for 2^+ states, using the values from

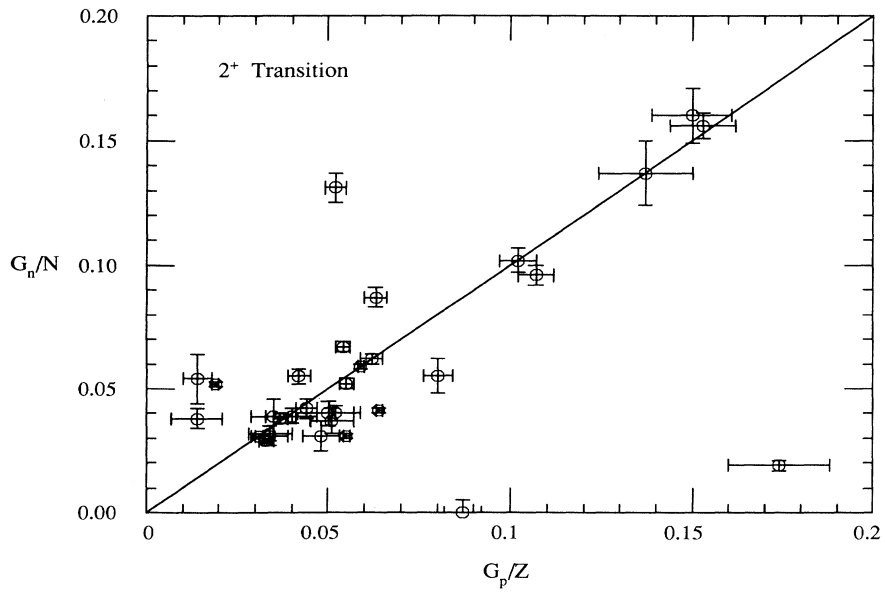

FIG. 9. As Fig. 8, but for 2^+ transitions to other than the lowest-lying states.

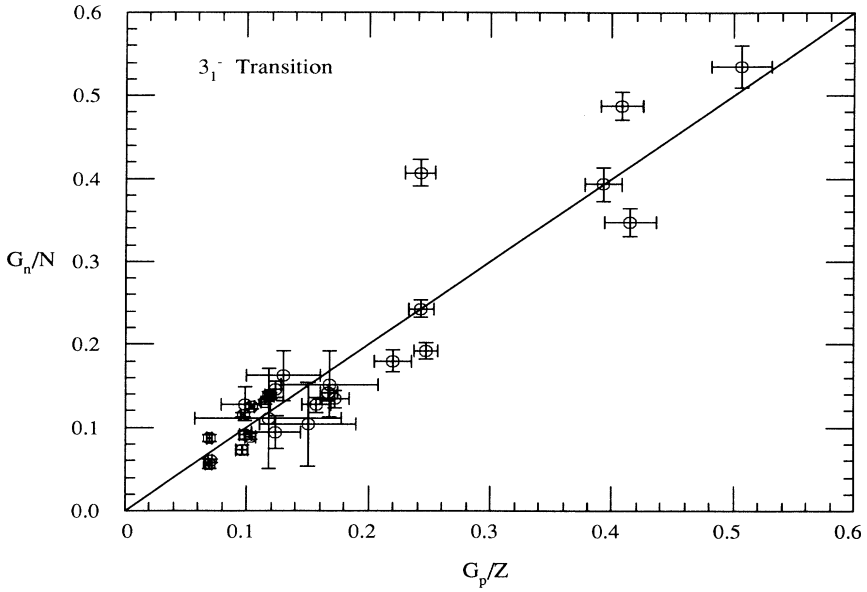

FIG. 10. As Fig. 8, but for the lowest-lying 3^- states.

Table I. Most of the instances are for the lowest 2^+ state. Over a wide range of strengths, these results are nearly equal. Isoscalar strengths to 3^- states, also mostly the lowest, are shown for pion and alpha particle scattering in Fig. 19. Again, the results are essentially the same for a wide range of strengths. An assumption of equality of matrix elements from pions and folding analyses of alpha particle scattering, using the data of Figs. 18 and 19, gives $\chi^2/N_{\rm dof}$ equal to 9.2 and 2.4 for the 2_1^+ and 3_1^- transitions, respectively.

Extractions of matrix elements from pion cross sections could have two roots, and the satisfactory comparison to alpha scattering shows that the correct solution has been presented, even in the many examples in Table I that did not use the folding method.

The pion data may also be treated to extract the isovector matrix elements for the nuclear transitions. These are directly available for excitation of a $T = 1$ level from a $T = 0$ ground state. The sole example of this available from pion data is for the 16.1 MeV 2^+ state of ^{12}C. As expected for an isospin symmetric reaction, the cross sections for π^+ and π^- are equal, and the proton matrix element agrees with that determined by electromagnetic transitions.

Other purely isovector matrix elements may be determined by charge exchange reactions to analogs of low-

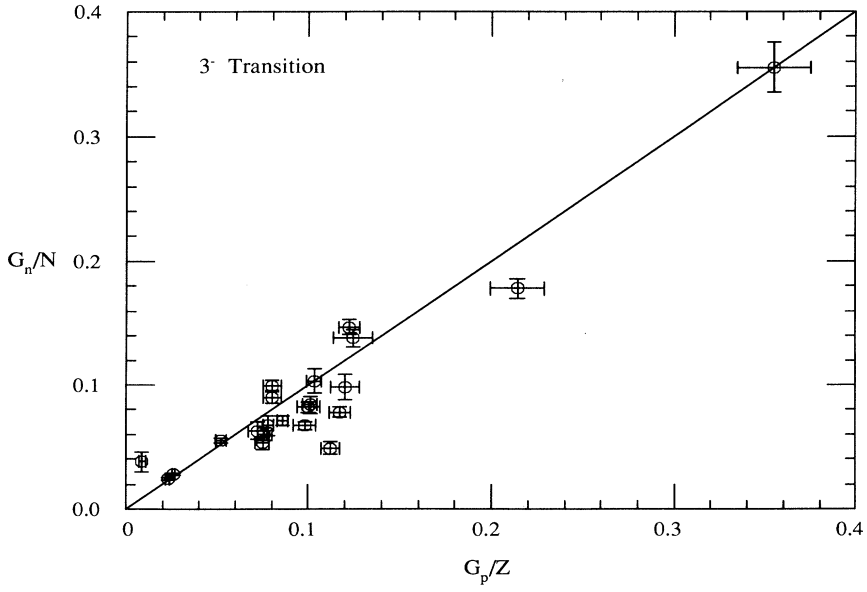

FIG. 11. As Fig. 8, but for 3^- transitions to other than the lowest-lying states.

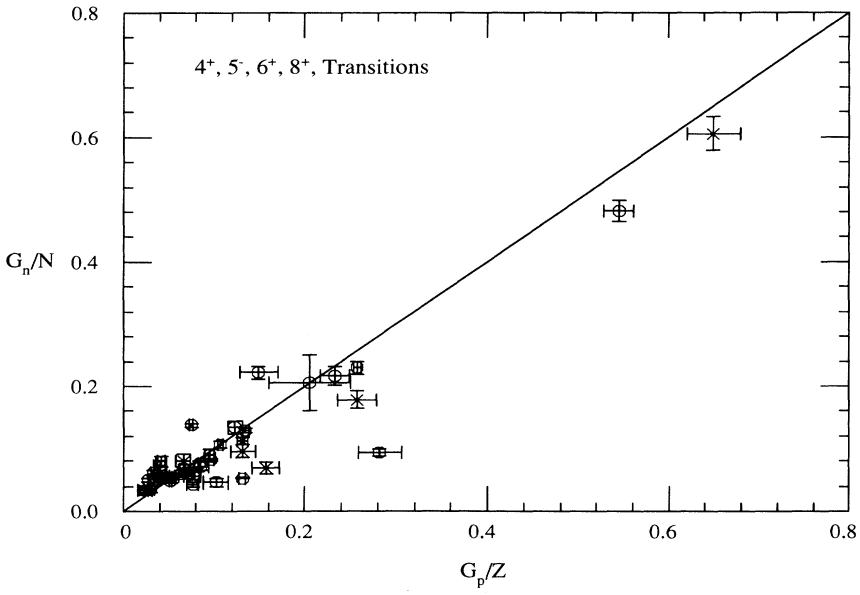

FIG. 12. As Fig. 8, but for multipolarities greater than three. Symbols are the same as used in Fig. 8.

lying states of the target. Some examples are included in Table I for heavy nuclei. A more detailed comparison has been made for ^{13}C, not included in the present work on zero spin targets [24].

A general comparison of the isospin properties of nuclear transitions from several probes is provided by four doubly even isotopes of Pd. The pion data [25] were initially compared to a specific nuclear model, and a more general analysis of these data followed [26]. Since then there are new isoscalar matrix elements from alpha particle scattering [15] and isovector matrix elements from the (p,n) charge exchange reaction [27]. Improved electromagnetic results are also available from the Coulomb excitation in the alpha scattering [15].

Figure 20 shows the isospin matrix elements inferred from the pion data for the first 2^+ states, with uncertainties as stated [25]. Vertical lines for each isotope indicate the M_0 values inferred from the alpha scattering of Ref. [15]. To account for the greater radius sensed by the alpha particle, these results have been scaled to match the pion data by a factor of $(1.2/1.4)^L$. Horizontal lines indicate the M_1 values from the (p,n) reaction [27]. These intersect very near the pion data points. The four slanted lines use the electromagnetic matrix elements to infer the relation between M_0 and M_1 for each isotope. These pass above the pion data for the

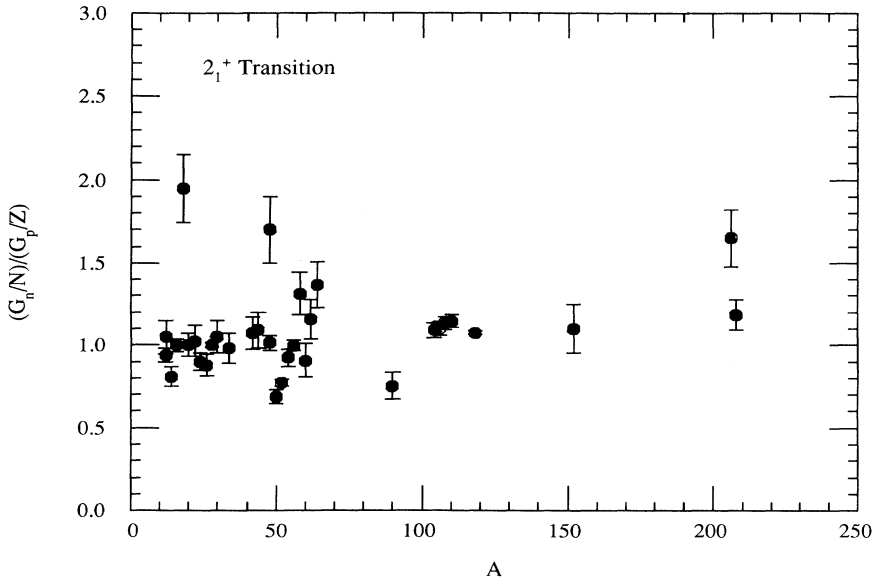

FIG. 13. The ratios of neutron to proton matrix elements, in SPU per nucleon, are plotted for the range of target masses studied for pion scattering to the first 2^+ transitions. A uniform hydrodynamic oscillation would give unity for this ratio.

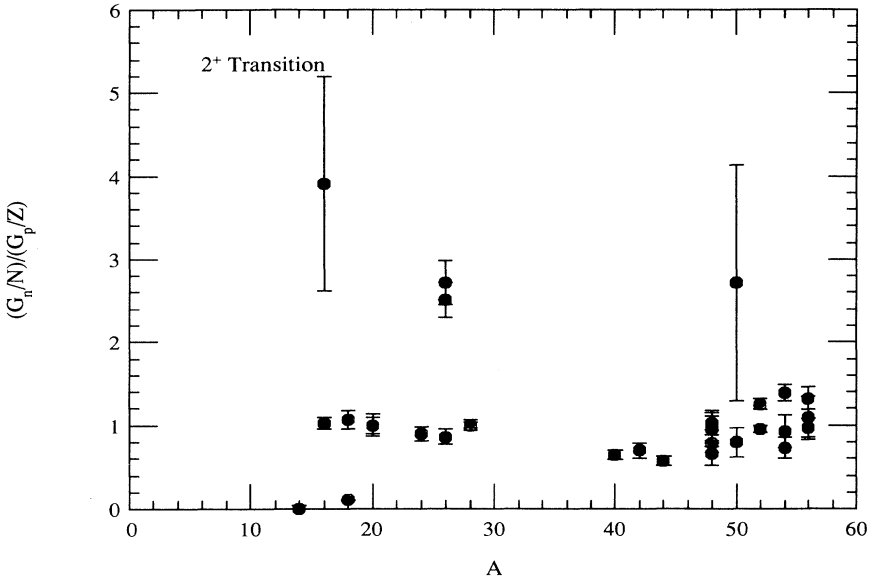

FIG. 14. As Fig. 13, but for 2^+ transitions to other than the first 2^+ state.

three lightest isotopes and below for the heaviest, without considering the uncertainties. The pion data show the smoothest progression of data points, possibly due to the fact that all four targets were in the same beam spot for greater relative reliability [25]. The heavy diagonal line shows the trend of M_1 values expected from the isoscalar values scaled in accord with the hydrodynamic model, $M_1 = (N-Z)M_0/A$. All four isotopes are slightly neutronlike, as seen by being above this curve.

In contrast to these agreements for the first 2^+ states of the Pd series, the pion data for the first 3^- states shown in Fig. 21 do not match the M_0 values from the rescaled alpha scattering results [15], nor do they match the short diagonal lines to show the relation between M_0 and M_1 to be inferred from the electromagnetic results. These are available for only three isotopes. The trend of the pion M_1 values is like the heavy diagonal line from the hydrodynamic model, but above it as evidence for a more neutronlike transition. The trends with isotopic mass are opposite for the first 2^+ and 3^- collective states of these Pd isotopes.

VI. BREAKING OF THE SYMMETRY

Almost all of the transitions dealt with are to bound states, and all except one are sharp states in the spectra. The exception is the 9.00 MeV fourth 2^+ state of ^{20}Ne, with an intrinsic width of 800 keV [28]. The sym-

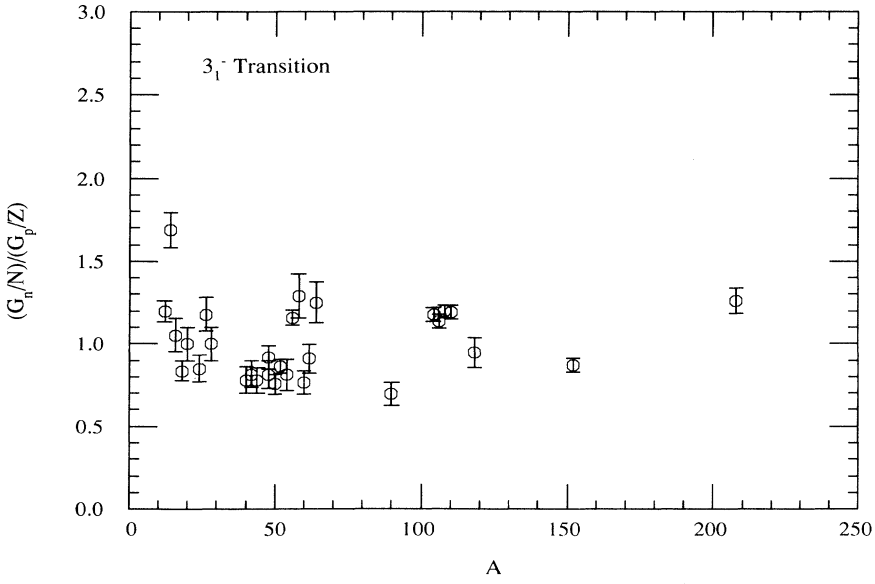

FIG. 15. As Fig. 13, but for transitions to the lowest-lying 3^- states.

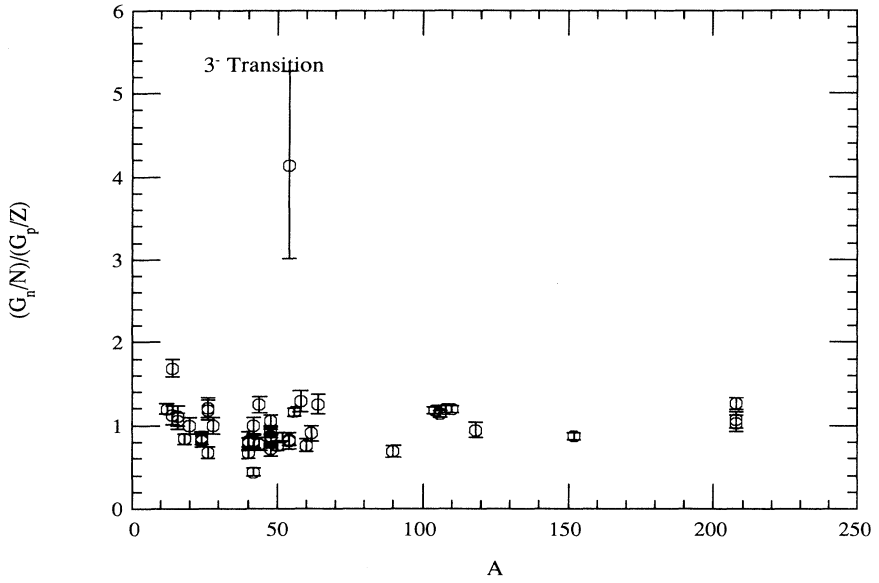

FIG. 16. As Fig. 13, but for all 3^- transitions, including those shown in Fig. 15.

metry between π^+ and π^- cross section still holds for this transition [29], to show that width or lifetime do not necessarily imply an asymmetry. This state decays by alpha particle emission, and is bound to both neutron and proton decays, which could be an expected source of an isospin symmetry breaking.

Some of the examples shown in the figures do not agree with the general trends and must be addressed individually. Agreements between proton matrix elements from pion scattering and charge matrix elements by electromagnetic studies must first be treated.

The compilation of Ref. [8] lists an electromagnetic transition probability for the 8.32 MeV second 2^+ state of ^{14}C that does not agree with the original presentation of the electron scattering data [30], which has been used in Table I and in Fig. 3. This original proton matrix element agrees with the pion result. The vanishing neutron matrix element noted in Fig. 9 for this transition has been treated in detail in Ref. [31]. A specific shell model is found to give better success than the bulk models used for the present comparisons.

Some of the data points falling off the diagonal lines in Figs. 2 and 4 are from a reanalysis of pion data on four Ni isotopes from Ref. [32]. An electronic gate was set to diminish the count rate from elastic scattering in many of the spectra of that work, and possible instabilities in that gate could influence the measurements of cross sections to the low-lying states shown for Ni. Uncertainties have been increased to 10% for the matrix elements in partial compensation for the problem.

The most collective transition noted in this work is for the first 2^+ state of deformed ^{152}Sm. A recent analysis [33] confirms the original results cited in Table I.

In Fig. 5 the 7.16 MeV 3^- transition in ^{20}Ne sits above the diagonal line that represents many of the results. This is a doublet in the electron scattering spectra, and

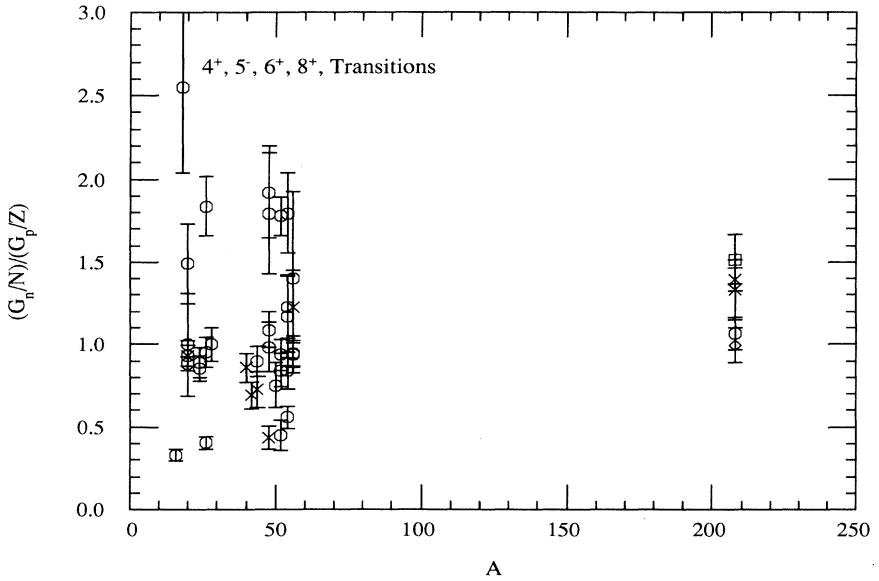

FIG. 17. As Fig. 13, but for multipolarities greater than three.

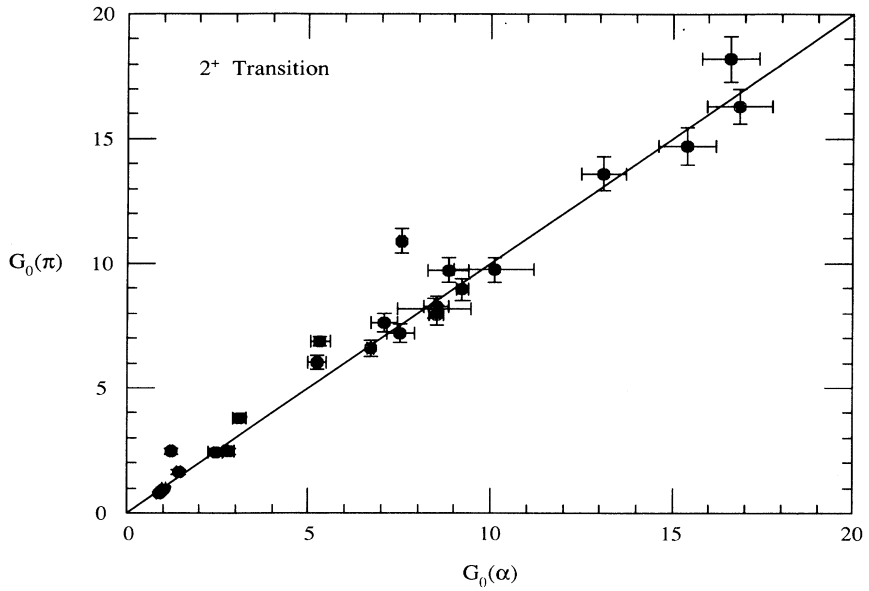

FIG. 18. Isoscalar matrix elements for 2^+ transitions are compared for pion scattering and folding model analyses of alpha particle scattering. Good agreement is found.

it is easy to ascribe more of the observed strength to the 3^- member, to increase the charge matrix element by as much as a factor of 1.5 [34]. This would improve the agreement with the pion data.

An unresolved doublet in ^{42}Ca includes the pion data for the first 5^- state of ^{42}Ca [35], shown by the cross above the diagonal line in Fig. 6. If the other member of the doublet has significant strength, this pion data point must drop to be nearer the diagonal.

The general trend of equal neutron and proton matrix elements per nucleon seen in Fig. 8 is not matched by the first 2^+ transition in ^{18}O. This is an example with a striking valence neutron configuration, which would give a zero proton matrix element in the most extreme model. A specific shell model calculation matches the data for this transition more closely than does the bulk model used in the present work [36]. A higher 2^+ state of ^{18}O at 5.26 MeV is far below the diagonal in Fig. 9, and has also been treated in Ref. [36]. The 8.32 MeV second 2^+ transition in ^{14}C also lies below the diagonal in Fig. 9, and has been considered in Ref. [31], as has the 3^- ^{14}C transition well above the diagonal line in Fig. 10. No pion data exist for the 2_2^+ state of $T = 1$ ^{34}S for comparison to electron scattering [59].

The point farthest from the diagonal line in Fig. 12 is for the 10.35 MeV 4^+ state of ^{16}O, well below the general trend. Perhaps the very high excitation energy makes the collective analysis inappropriate.

Higher 2^+ states may reverse the isospin asymmetry of the first 2^+ state in certain nuclei. Several of the data points off the diagonal lines in Fig. 9 are in ^{26}Mg and ^{18}O, where such effects have been anticipated [19].

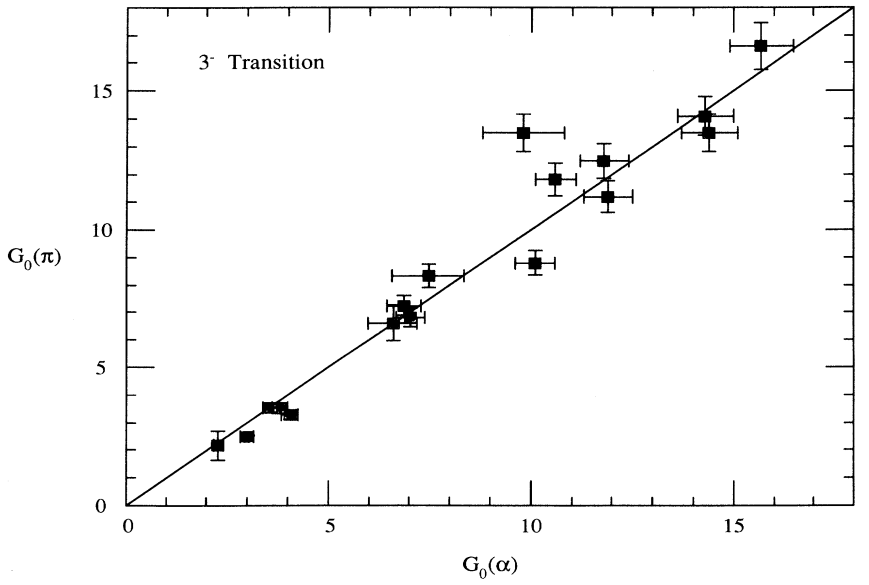

FIG. 19. As Fig. 18, but for 3^- transitions of a range of nuclei.

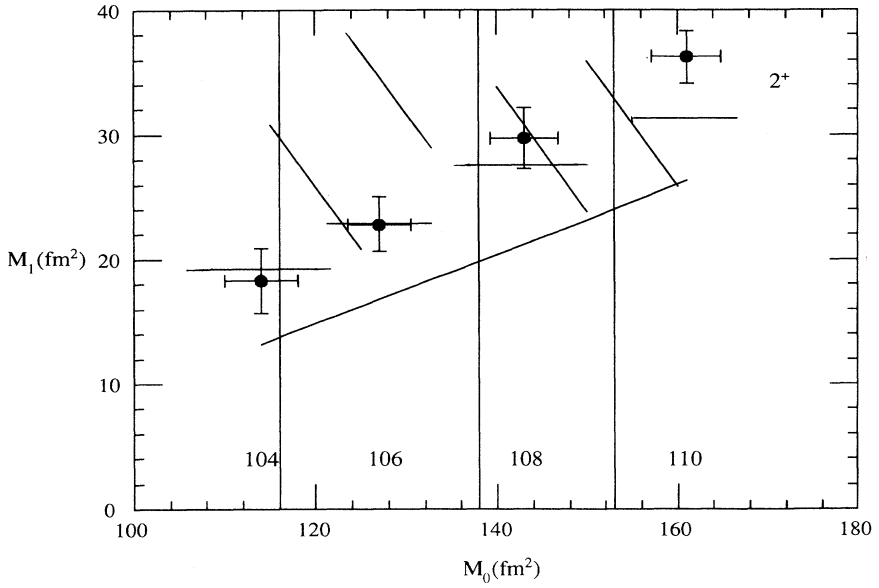

FIG. 20. Isoscalar and isovector matrix elements inferred from pion scattering to the first 2^+ states of the even Pd isotopes are compared to the expectation of the hydrodynamic model. Data are from Saha *et al.* [25]. Isoscalar strengths inferred from alpha particle scattering [15] are shown as vertical lines, while isovector strengths inferred by charge exchange to analogs of these states are shown as horizontal lines [27]. The relation between M_0 and M_1 fixed by the electromagnetic strength is shown for each isotope by the diagonal lines. The long diagonal line shows the relation between M_1 and M_0 expected from the hydrodynamic ratio of $(N - Z)/A$.

The special case of ^{48}Ca, with its large neutron excess and closed shells, has been considered in Ref. [37]. The neutronlike first 2^+ transition for ^{48}Ca seen in Fig. 13 is in concord with this theory. The first 3^- state is expected to have a hydrodynamic response, as is found in the data point found for ^{48}Ca in Fig. 15. A prediction that the second 3^- state be neutronlike is not confirmed by the data point for ^{48}Ca in Fig. 17.

Exceptions from the hydrodynamic trend are also seen for higher 2^+ states of ^{16}O, ^{26}Mg, and ^{50}Ti in Fig. 14. The uncertainties reflect the weak strengths of these transitions in targets with at least one closed shell. The greatest difference from the hydrodynamic model result is seen for the 5.62 MeV second 3^- state in ^{54}Fe in Fig. 16. This exception has a proton matrix element of but 0.26 single particle unit.

Second-order scattering processes for pions could be important for weak higher states in collective nuclei, but

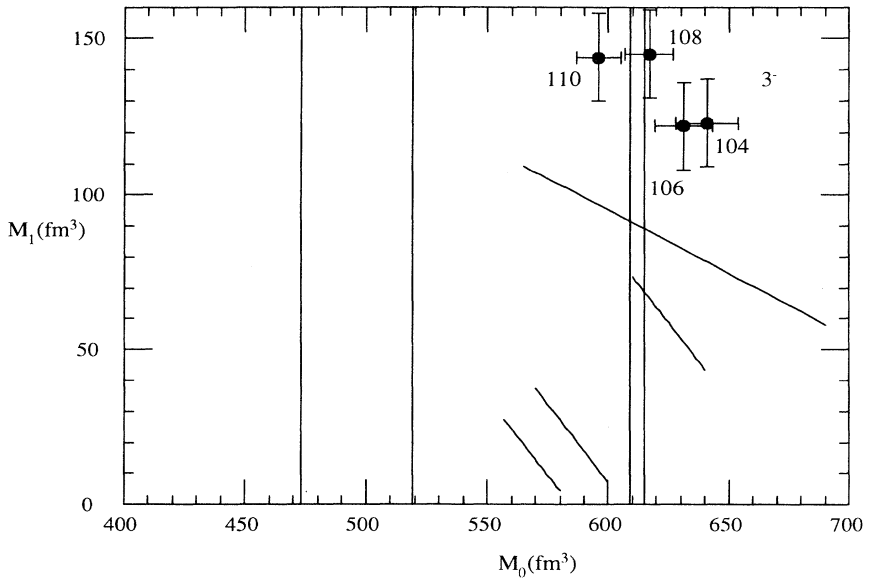

FIG. 21. As Fig. 20 for the first 3^- states of the even Pd isotopes.

have not been considered here. It may be noted in Fig. 3 that weak proton amplitudes inferred by pion scattering are often above those found by electromagnetic transitions. This may indicate a need to consider a higher-order reaction model.

In Fig. 4 the well-measured datum for the 9.6 MeV 3^- state in ^{12}C lies below the diagonal line, with only a first-order analysis for the pion data. A second-order model may be needed, or perhaps the folding of radial distributions is not treated adequately for this high multipolarity in the lightest nucleus considered in this work.

Most of the exceptions from the general "hydrodynamic" trend of isospin symmetry are thus found to have explanations or to have likely differences in the reaction mechanism. It is that symmetry that remains the most striking feature of the large data set of low-lying nuclear transitions.

Giant resonance transitions, above nucleon emission thresholds, do show a breakdown of the isospin symmetry so prominent in the data shown in the present work [38, 39]. Alternative explanations not appropriate for the states bound to nucleon decay must be considered, and the giant resonance results do not contradict the conclusions of this survey.

VII. RECAPITULATION

A large and wide range of pion data has been analyzed and compiled to yield nuclear transition matrix elements for proton and neutron amplitudes and for their isoscalar and isovector combinations. Proton and charge matrix elements are found to be in good agreement for many cases, although evidence for multistep reactions is suggested for some weak transitions. Neutron matrix elements for the first 2^+ states determined by several means are in satisfactory agreement with the pion results as well. Only when alpha particle scattering data are analyzed by a folding model do the isoscalar amplitudes agree with those from the pion work. This is presumably because of the imperative to treat the radial distributions carefully for the composite scattering probe. Most alpha particle results listed in Table I do not use this model, and have not been presented in figures. A more thorough analysis on these cases could be made to tighten the comparison to the pion scattering results. The very few direct comparisons of isovector matrix elements for pions to other determinations are found to agree.

This satisfying situation is in part due to the self-selecting nature of the cases available for comparison. Strongly collective transitions are most readily seen in the inelastic scattering spectra, and these are also the ones most suited to the bulk vibrational nuclear model for the transitions used throughout this work.

The important result of this work is the tracking of the ratios M_n/M_p with N/Z, as expected in the simplest bulk models for nuclear transitions. This dynamic symmetry has been noted for many individual cases, but has now been shown to be valid in general. A simple explanation would be the high degree of isoscalar collective ordering and correlations for natural parity low-lying states, as noted long ago [1].

ACKNOWLEDGMENTS

Thanks are extended to D. Oakley for assistance in the DWIA calculations and to S. Parry for generating the many figures. All of the data presented were taken with the EPICS pion spectrometer at LAMPF, designed and built by H. A. Thiessen and ably improved and operated by the MP10 group, headed by R. L. Boudrie.

[1] A. M. Bernstein, Adv. Nucl. Phys. **3**, 325 (1969).
[2] V. A. Madsen and V. R. Brown, Phys. Rev. Lett. **52**, 176 (1984).
[3] C. L. Morris, Phys. Rev. C **13**, 1755 (1976).
[4] D. S. Oakley, P. D. Kunz, and C. L. Morris, Phys. Rev. C **41**, 1081 (1990).
[5] H. DeVries, C. W. DeJaeger, and C. DeVries, At. Data Nucl. Data Tables **36**, 495 (1987).
[6] W. B. Cottingame *et al.*, Phys. Rev. C **36**, 230 (1987).
[7] G. Rowe, M. Salomon, and R. H. Landau, Phys. Rev. C **18**, 584 (1979).
[8] R. A. Eisenstein and G. A. Miller, Comput. Phys. Commun. **11**, 95 (1976).
[9] S. Raman, C. H. Malarkey, W. T. Minor, C. W. Nestor, and P. H. Stelson, At. Data Nucl. Data Tables **36**, 1 (1987).
[10] P. M. Endt, At. Data Nucl. Data Tables **23**, 3 (1979); Nucl. Phys. **A521**, 1 (1990).
[11] P. M. Endt, At. Data Nucl. Data Tables **23**, 547 (1979).
[12] DWUCK4, a zero-range distorted-wave Born approximation code available from P. D. Kunz, University of Colorado (unpublished).
[13] A. M. Bernstein, V. R. Brown, and V. A. Madsen, Phys. Rev. Lett. **42**, 425 (1979).
[14] T. K. Alexander, B. Castel, and I. S. Towner, Nucl. Phys. **A445**, 189 (1985).
[15] V. Riech, R. Scherwinski, G. Lindstrom, E. Fretwurst, K. Gridnev, P. P. Zarubin, and R. Kolalis, Nucl. Phys. **A542**, 61 (1992).
[16] M. M. Gazzaly, N. M. Hintz, G. S. Kyle, R. K. Owen, G. W. Hoffmann, M. Bartlett, and G. Blanpied, Phys. Rev. C **25**, 408 (1982).
[17] C. S. Whisnant, Phys. Rev. C **40**, 1744 (1989).
[18] D. S. Oakley and H. T. Fortune, Phys. Rev. C **35**, 1392 (1987).
[19] V. R. Brown, A. M. Bernstein, and V. A. Madsen, Phys. Lett. **164B**, 217 (1985).
[20] D. S. Oakley *et al.*, Phys. Rev. C **44**, 2058 (1991).
[21] N. M. Hintz *et al.*, Phys. Rev. C **45**, 601 (1992).
[22] C. L. Morris *et al.*, Phys. Rev. C **35**, 1388 (1987).
[23] D. J. Horen *et al.*, Phys. Lett. B **296**, 18 (1992).
[24] R. J. Peterson, J. R. Shepard, and R. A. Emigh, Phys. Rev. C **24**, 826 (1981).
[25] A. Saha, K. K. Seth, D. Godman, D. Kielczewska, R. Seth, J. Stuart, and O. Scholten, Phys. Lett. **132B**, 51 (1983).

[26] H. T. Fortune, J. Phys. G **11**, 1305 (1985).
[27] J. D. Anderson *et al.*, Phys. Rev. C **41**, 1993 (1990).
[28] F. Ajzenburg-Selove, Nucl. Phys. **A475**, 1 (1987).
[29] M. Burlein *et al.*, Phys. Rev. C **40**, 785 (1989).
[30] H. Crannell, P. L. Hallowell, J. T. O'Brien, J. M. Finn, F. J. Kline, S. Penner, J. W. Lightbody, and S. P. Fivozinsky, in Supplement to the Research Report of Laboratory of Nuclear Science, Tohoku University, 1972, Vol. 5, p. 375.
[31] A. C. Hayes *et al.*, Phys. Rev. C **37**, 1554 (1988).
[32] D. S. Oakley, M. R. Braunstein, J. J. Kraushaar, R. A. Loveman, R. J. Peterson, D. J. Rillett, and R. L. Boudrie, Phys. Rev. C **40**, 859 (1989).
[33] J. Bartel, M. B. Johnson, M. K. Singham, and W. Stocker, Phys. Lett. B **296**, 5 (1992).
[34] R. P. Singhal, H. S. Caplan, J. R. Moreira, and T. E. Drake, Can. J. Phys. **51**, 2125 (1973).
[35] K. G. Boyer, Los Alamos Report LA-9974-T, 1984.
[36] S. Chakravarti, D. Dehnhard, M. A. Franey, S. J. Seestrom-Morris, D. B. Holtkamp, C. L. Blilie, A. C. Hayes, C. L. Morris, and D. J. Millener, Phys. Rev. C **35**, 2197 (1987).
[37] J. R. Vanhoy, M. T. McEllistrem, S. F. Hicks, R. A. Gatenby, E. M. Baum, E. L. Johnson, G. Molnar, and S. W. Yates, Phys. Rev. C **45**, 1628 (1992).
[38] J. L. Ullmann *et al.*, Phys. Rev. C **35**, 1099 (1987).
[39] S. J. Seestrom-Morris, C. L. Morris, J. M. Moss, T. A. Carey, D. Drake, J. C. Dousse, L. C. Bland, and G. S. Adams, Phys. Rev. C **33**, 1847 (1986).
[40] D. B. Holtkamp, S. J. Seestrom-Morris, D. Dehnhard, H. W. Baer, C. L. Morris, S. J. Greene, C. J. Harvey, D. Kurath, and J. A. Carr, Phys. Rev. C **31**, 957 (1984).
[41] R. J. Peterson, H. C. Bhang, J. J. Hamill, and T. G. Masterson, Nucl. Phys. **A425**, 469 (1984).
[42] C. L. Blilie, D. Dehnhard, M. A. Franey, D. H. Gay, D. B. Holtkamp, S. J. Seestrom-Morris, P. J. Ellis, C. L. Morris, and D. J. Millener, Phys. Rev. C **30**, 1989 (1984).
[43] D. B. Holtkamp, Ph.D. thesis, University of Texas at Austin; Los Alamos Report LA 8231-T, 1980.
[44] H. Rebel, Z. Phys. A **277**, 35 (1976).
[45] S. Seestrom-Morris, D. Dehnhard, M. A. Franey, D. B. Holtkamp, C. L. Blilie, C. L. Morris, J. D. Zumbro, and H. T. Fortune, Phys. Rev. C **37**, 2057 (1988).
[46] S. G. Iversen, Ph.D. thesis, University of Texas at Austin; Los Alamos Report LA 7828, 1979.
[47] D. M. Manley *et al.*, Phys. Rev. C **43**, 2147 (1991).
[48] M. Burlein, Ph.D. thesis, University of Pennsylvania; Los Alamos Report LA-11697-T, 1989.
[49] H. J. Gils and H. Rebel, Z. Phys. A **274**, 259 (1975).
[50] J. Fritze, R. Neu, H. Abele, F. Hoyler, G. Staudt, P. D. Eversheim, F. Hintenberger, and H. Muther, Phys. Rev. C **43**, 2307 (1991).
[51] G. S. Blanpied *et al.*, Phys. Rev. C **41**, 1625 (1990).
[52] A. Johnston and T. E. Drake, J. Phys A **7**, 898 (1974).
[53] K. van der Borg, M. N. Harakeh, and A. van der Woude, Nucl. Phys. **A365**, 243 (1981).
[54] R. Neu, S. Welte, H. Clement, H. J. Hauser, G. Staudt, and H. Muther, Phys. Rev. C **39**, 2145 (1989).
[55] E. W. Lees, A. Johnston, S. W. Brain, C. S. Curran, W. A. Gillespie, and R. P. Singhal, J. Phys. A **7**, 936 (1974).
[56] M. McKinzie *et al.*, Bull. Am. Phys. Soc. **37**, 1303 (1992).
[57] C. Olmer *et al.*, Phys. Rev. C **21**, 254 (1980).
[58] S. Roy, T. Dey, A. Goswami, S. N. Chintalapudi, and S. R. Banerjee, Phys. Rev. C **45**, 2904 (1992).
[59] U. Worsdorfer, H. J. Emrich, H. Miska, and D. Rychel, Nucl. Phys. **A438**, 711 (1985).
[60] A. Saha, K. K. Seth, M. Artuso, B. Harris, R. Seth, H. Nann, and W. W. Jacobs, Phys. Rev. Lett. **52**, 1876 (1984).
[61] K. G. Boyer *et al.*, Phys. Rev. C **24**, 598 (1981).
[62] K. Itoh, Y. M. Shin, W. J. Gerace, and Y. Torizuka, Nucl. Phys. **A492**, 426 (1989).
[63] R. J. Peterson, Ph.D. thesis, University of Washington, 1966, unpublished.
[64] S. Mordechai *et al.*, Phys. Rev. C **36**, 1950 (1987).
[65] J. Heisenberg, J. S. McCarthy, and I. Sick, Nucl. Phys. **A164**, 353 (1971).
[66] P. M. Endt, Nucl. Phys. **A521**, 1 (1990).
[67] J. M. Wise, Ph.D. thesis, University of Virginia, 1982, unpublished.
[68] D. S. Oakley *et al.*, Phys. Rev. C **35**, 1392 (1987); D. S. Oakley, Ph.D. thesis, University of Texas at Austin; Los Alamos Report LA 10968-T, 1987.
[69] P. M. Endt, At. Data Nucl. Data Tables **23**, 547 (1979).
[70] A. M. Bernstein, Nucl. Phys. **A115**, 79 (1968).
[71] T. Guhr, H. Diesener, A. Richter, C. W. deJager, H. de Vries, and P. K. A. deWitt Huberts, Z. Phys. A **336**, 159 (1990).
[72] P. X. Ho, J. Bellicard, P. Leconte, and I. Sick, Nucl. Phys. **A210**, 189 (1973).
[73] J. Yntema and G. R. Satchler, Phys. Rev. **161**, 1137 (1967).
[74] J. W. Lightbody *et al.*, Phys. Rev. C **27**, 113 (1983).
[75] K. Maeda, H. Orihara, T. Murakami, S. Nishihara, K. Miura, and H. Ohnuma, Nucl. Phys. **A403**, 1 (1983).
[76] F. E. Bertrand, G. R. Satchler, D. J. Horen, J. R. Wu, A. D. Bacher, G. T. Emery, W. P. Jones, D. W. Miller, and A. van der Woude, Phys. Rev. C **22**, 1832 (1980).
[77] A. A. Cowley, P. M. Cronje, G. Heymann, S. J. Mills, and J. vanStaden, Nucl. Phys. **A229**, 256 (1974).
[78] M. R. Braunstein, J. J. Kraushaar, R. P. Michel, J. H. Mitchell, R. J. Peterson, H. P. Blok, and H. deVries, Phys. Rev. C **37**, 1870 (1988).
[79] M. Lahanas, D. Rychel, P. Singh, R. Gyufko, D. Kolbert, B. van Kruchten, E. Madadakis, and C. A. Wiedner, Nucl. Phys. **A455**, 399 (1986).
[80] R. J. Peterson, J. J. Kraushaar, M. R. Braunstein, and J. H. Mitchell, Phys. Rev. C **44**, 136 (1991).
[81] C. L. Morris, S. J. Seestrom-Morris, P. A. Seidl, R. R. Kiziah, and S. J. Greene, Phys. Rev. C **28**, 2165 (1983).
[82] E. I. Obiajunwa, L. H. Rosier, and J. van der Wiele, Nucl. Phys. **A500**, 341 (1989).
[83] D. J. Horen *et al.*, Phys. Rev. C **46**, 499 (1992).
[84] R. G. Helmer, Nucl. Data Sheets **61**, 93 (1990).
[85] M. G. Martin, Nucl. Data Sheets **47**, 797 (1986).